FH University of Applied Sciences
TECHNIKUM WIEN

MASTER THESIS

Thesis submitted in partial fulfillment of the requirements for the degree of Master of Science in Engineering at the University of Applied Sciences Technikum Wien - Degree Program Medical Engineering & eHealth

By: Martin Bečička, Bsc et Bsc

Student Number: 2210228030

Supervisors: Ing. Richard Paštěka, Msc
prof. MUDr. Julie Dobrovolná, Ph.D.

Wien, May 18, 2023

Declaration

“As author and creator of this work to hand, I confirm with my signature knowledge of the relevant copyright regulations governed by higher education acts (see Urheberrechtsgesetz /Austrian copyright law as amended as well as the Statute on Studies Act Provisions / Examination Regulations of the UAS Technikum Wien as amended).

I hereby declare that I completed the present work independently and that any ideas, whether written by others or by myself, have been fully sourced and referenced. I am aware of any consequences I may face on the part of the degree program director if there should be evidence of missing autonomy and independence or evidence of any intent to fraudulently achieve a pass mark for this work (see Statute on Studies Act Provisions / Examination Regulations of the UAS Technikum Wien as amended).

I further declare that up to this date I have not published the work to hand nor have I presented it to another examination board in the same or similar form. I affirm that the version submitted matches the version in the upload tool.“

Wien, May 18, 2023

Signature

Elektronicky podepsáno
Martin Bečička

09:55 18.05.2023
RSA/4096

Abstract

Over the past few decades, numerous models have been created to estimate human thermal responses. These models rely on energy balance equations that consider the heat exchange between the human body and its environment. These models have substantially progressed from one-node models into complex structures organized in multiple layers and connected by a circulatory blood flow. Although there is literature available comparing the possible utility of the thermophysiological models in different scenarios, little is known about the utility of these models in specific conditions. This work investigates and compares selected thermophysiological models, focusing on selecting a suitable model for the use case scenario of Antarctica.

The data was collected during a longitudinal study located at Johann Gregor Mendel Czech Antarctic station. The local skin temperature of participants (n = 16) was measured 6 times over the period of the study. The first of each measurement set consisted of orthostatic tests in addition to psychomotor vigilance task and Iowa gambling test present which were present in each of the subsequent measurements.

After examining specific experimental conditions, four thermophysiological models were compared, and the JOS-3 model was determined to be the most appropriate for the thermal data obtained during the experiment.

The results revealed that the selected JOS-3 model can accurately predict mean skin temperatures for both experiment designs (RMSD 0.72 and 0.75 °C for experiment design 1 and 2 respectively). Furthermore, the JOS-3 model was able to reliably predict head (RMSD 0.82 and 1.13 °C), neck (RMSD 0.61 and 1 °C), and chest (RMSD 1.01 and 1.22 °C) skin temperatures. However, deviations observed for back, hand, and foot segments were significant (RMSD 2.08 - 2.25 and 2.55 - 2.68 °C). Possible explanations include uncertainty in clothing insulation of the worn clothing, uncertainty in measurement circumstances (contact with surfaces - floor, table), and the placement of the thermal sensors. The highest deviation was observed in the pelvis (RMSD 2.25 and 3.72 °C) and is possibly a result of the JOS-3 model overestimation of heat production in the segment. The study has underscored the significance of obtaining comprehensive data on clothing type and sensor placement for enhancing the accuracy of simulation outcomes.

Keywords: thermophysiological model, thermal comfort, local skin temperature

Acknowledgements

I would like to express my deepest gratitude to my two supervisors, prof. MUDr. Julie Dobrovolná, Ph.D., and Ing. Richard Paštěka, Msc, for their invaluable support and guidance throughout my diploma thesis. Their expertise, encouragement, and constructive feedback have been instrumental in shaping my diploma thesis.

Additionally, I would like to extend my heartfelt appreciation to Mgr. et Mgr. Filip Zlámal, Ph.D., who assisted me with a plethora of questions and obstacles I encountered during the creation of my thesis. His expertise and desire to help were of great value to me along the way.

Finally, I would like to extend my thanks to all the participants who took part in the research, without whom this thesis would not have been possible.

Contents

1 Introduction

Thermal comfort is a crucial aspect in assessing indoor and outdoor environmental conditions that ultimately affect health, productivity, and overall well-being. As such thermal comfort has been a subject of intensive effort by the scientific community to quantify the conditions in which humans feel thermally comfortable.

The field of thermal comfort naturally evolved from assessing thermally neutral conditions to modeling the whole human thermophysiological system with all the complexities involved. These models are known as thermophysiological models and aim to faithfully represent temperature responses to various environmental conditions. At present, there are many practical applications of thermophysiological models such as simulating and designing suitable microclimatic conditions i.e. car cabins, airplane cabins, indoor environments, or even space suits. Optimizing environmental conditions can also lead to reducing energy requirements and can be cost-effective.

Although models have been validated for a general scenario frequently obtained in strictly controlled conditions specifically for the study, the literature is lacking a comprehensive thermophysiological models accuracy comparison for the same experiments. Therefore little is usually known about the accuracy of any model under specific experimental conditions. Furthermore, experiments validating thermophysiological models are done on relatively long time frames, such as 2 - 3 hours, and the accuracy of these models on shorter time frames is not well established.

The objective of this work is to select a suitable thermophysiological model for the experimental data obtained in Antarctica and evaluate its accuracy in the specific environmental conditions and other conditions specific to the conducted experiment.

1.1 Thermal Regulation in Humans

Humans belong to the group of endothermic homeotherms. Endothermic means that they can maintain body temperature by producing metabolic heat when needed. Homeothermic means the internal body temperature is maintained despite much larger variations in the temperature of the environment. Even when the body is at rest thermoregulatory system is working hard to maintain a balance between heat gain and heat loss to the environment. Thermal regulatory loops need to constantly balance heat transfer with the environment with internal heat production. This is by no means a simple task a plethora of variables come into play. [1]

Heat is generated mainly through the oxidation of macronutrients such as proteins, fats, and

carbohydrates. The amount of energy spent on these heat-generating life-sustaining processes is known as basal metabolic rate (BMR). BMR is determined by measuring a resting, awake, and fasting individual. Metabolic rate increases proportionately to the intensity of physical exercise, posture, or even with the intensity of mental load. It also varies based on gender and has a decreasing tendency with progressing age. [1]

If the body is unable to maintain the physiological temperature range, adverse effects can occur. Specifically, high fever or hyperthermia 41 °C can cause denaturation of proteins, which can interfere with their function and lead to decreased efficiency of important biochemical processes such as oxidative phosphorylation. If untreated it can lead to severe dehydration, seizures, organ failures, and death. [1]

1.2 Thermogenesis

In humans, about 90 % of the energy consumed in the form of macronutrients can be metabolized. The rest is lost during digestion (4-8%) or is excreted through urine and the skin (3-5%). Metabolized energy is either used during the day or can be stored for later. One of the ways to quantify average daily expanded energy is the average daily metabolic rate (ADMR). ADMR consists of several components which can vary between the individuals depending on the amount of their physical activity, the environmental conditions, age, etc. Considering those variables to be average the ADMR consists of basal metabolic rate (55-65%), physical activity energy expenditure (25-35%), and lastly diet-induced thermogenesis (10%). [2]

All of the aforementioned components of ADMR produce heat as a byproduct and the heat generated is transferred to the environment which acts as a heat sink. In cold environments, the main focus of the body is to retain the heat produced inside the body and to produce more heat. More heat can be produced by shivering thermogenesis and non-shivering thermogenesis. Cold environments also cause discomfort and produce behavioral changes such as increasing clothing insulation, changing the environment, or starting a fire. [2]

In general, humans have a good ability to dissipate heat in hot environments. However, they are maladjusted in retaining and mainly producing heat when exposed to a cold environment. If not properly protected through shelter and clothing, exposure to cold environments can quickly lead to loss of body functions, permanent cell damage, and in more severe cases even death. [2]

1.2.1 Basal Metabolic Rate

Basal metabolic rate (BMR) is the energy expenditure required to maintain physiological functions (breathing, blood circulation, organ function) and for the organism to stay alive. BMR is measured on a fasting resting participant who is in a neutral thermal environment most commonly with indirect calorimetry. In terms of ADMR, it is usually its major component and remains

fairly constant day to day. Further delineation of components of BMR can be seen in figure 1. [3]

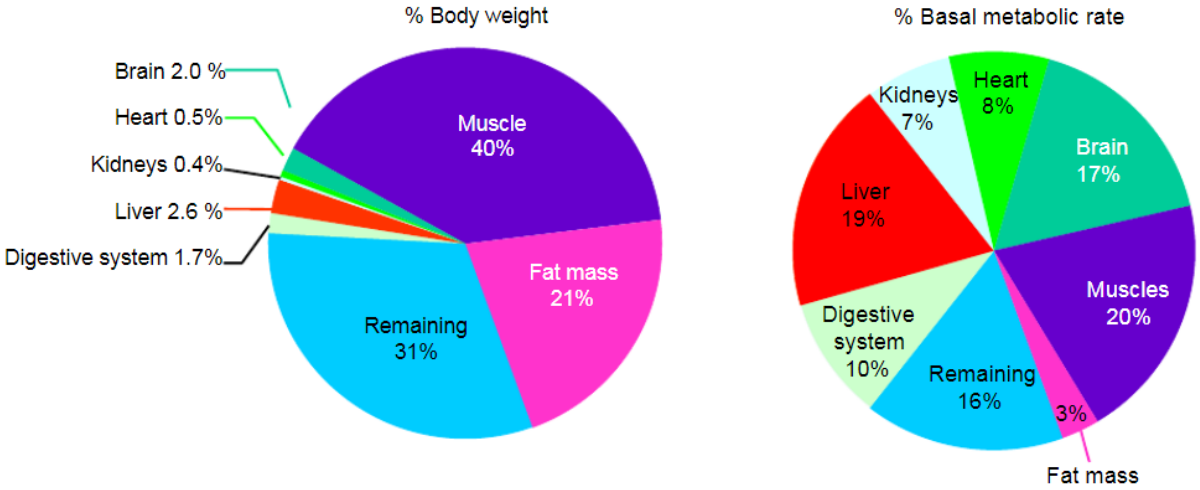

Figure 1: Components of BMR by tissue type [3].

BMR may be estimated through predictive equations, which consider several individual physiological characteristics. These include sex, weight, height, and age. Males generally have higher BMR values. BMR is expressed in terms of units of energy per unit of time, frequently in kJ per day. [3]

1.2.2 Thermic Effect of Food

The thermic effect of food (TEF) is the amount of energy required by the body to break down, process, and absorb nutrients from food. In terms of total energy expenditure, the TEF accounts for about 10%. The amount of energy required for TEF varies depending on the macronutrient content of the food. It has been measured that proteins have the highest TEF, requiring more energy when compared to carbohydrates and fat. The TEF of carbohydrates and fat are roughly the same, but about half the amount of carbohydrates. [4]

1.2.3 Activity Energy Expenditure

Energy expended on activities can be either non-exercise activity thermogenesis or exercise activity thermogenesis. The non-exercise activity thermogenesis refers to the energy expenditure that occurs during physical activity outside of structured exercise. It encompasses all the movement and activity performed during daily life and encompasses activities such as fidgeting, standing, walking, and household chores. [3]

1.2.4 Shivering Thermogenesis

During shivering thermogenesis heat is generated by involuntary muscle contractions, the intensity of the contractions is related to the duration and severity of cold exposure. Muscles convert chemical energy which is stored as ATP into kinetic energy. Shivering thermogenesis can amount to roughly 15% of the daily energy consumption. Shivering is a short-term adaptation and cannot be maintained over long periods. [2]

1.2.5 Non-shivering Thermogenesis

Non-shivering thermogenesis uses brown adipose tissue (BAT), more commonly referred to as brown fat. BAT is rich in mitochondria which normally produce ATP but can also through uncoupling proteins dissipate the proton gradient so the energy from the oxidation of fatty acids produces heat instead of ATP. Non-shivering and shivering thermogenesis were shown to be coupled and usually occur simultaneously. [2]

1.3 Heat Exchange with the Environment

The human body is constantly generating heat as a result of various life-sustaining processes, and it is essential to regulate the body temperature to maintain health and well-being. The human body exchanges heat with the environment through four mechanisms: radiation, convection, conduction, and phase change. These mechanisms allow the body to lose or gain heat, depending on the environmental conditions. The phase change from liquid to gas during evaporation is an important mechanism for heat exchange, as energy in the form of heat is absorbed from the body or environment to power the phase change. Other phase changes do not usually contribute significantly to heat exchange with the environment. [5]

Radiation is the transfer of heat through electromagnetic waves. Energy is exchanged through photons. Unlike conduction or convection transfer of heat through radiation does not require a medium and can occur even inside a vacuum. All objects with temperatures above absolute zero have thermal energy. Even though the electromagnetic spectrum is wide, objects with relatively low temperatures emit overwhelmingly in the infrared part of the spectrum. One notable difference is the sun. Reaching temperatures above 5,500 K most of the energy is emitted in the visible part of the spectrum. To demonstrate the relative importance of radiation compared to other mechanisms, a person standing inside a room with an ambient temperature of 20 C° with low airspeed, would transfer most heat to the environment by radiation. [5]

Heat transfer through **convection** can occur in a gas or a liquid. When fluid or gas is heated density lowers and starts to rise, when cooled the density rises and the gas or liquid starts to sink. As the liquid or gas moves it takes the heat with it resulting in heat transfer through convection. [5]

Heat transfer through **conduction** occurs when two objects are in physical contact and is realized on a molecular level. Molecules on the surface of the hotter object bump and transfer energy to the surface of the colder object. [5]

Heat exchange through **evaporation** is a process where heat is dissipated into space by the conversion of water to gas. Evaporation is part of the latent heat exchange and takes place on the skin or in the respiratory tract. Skin is the largest organ of the body and contains a plethora of sweat glands. Sweating is one of the chief ways our bodies lose heat when in hot environments. The rate of evaporation is dependent on the partial water vapor pressure in the location and on the temperature of the surrounding air. [5]

All of the types of heat transfer can and usually do occur simultaneously nevertheless the relative importance depends on the specific conditions.

1.4 Thermal Comfort

According to the American Society of Heating, Refrigerating and Air-Conditioning Engineers (ASHRAE) thermal comfort is defined as "Thermal comfort is that condition of mind that expresses satisfaction with the thermal environment" [6]. Hensen defines thermal comfort as "a state in which there are no driving impulses to correct the environment by the behavior" [7].

Regardless of the source of the definition, thermal comfort is a subjective experience that is influenced by an individual's current psychological state, cultural background, and various social influences. It is important that conventionally there is a difference between thermal comfort and thermal sensation. While the former has been defined as subjective, thermal sensation is treated as an objective sensation. If an ice cube was put on a forearm the thermal sensation would be cold, nevertheless from the standpoint of thermal comfort there individual might not be feeling overall thermal discomfort as the ambient temperature of the room is 21 °C. [8]

Although there is no absolute standard for measuring thermal comfort, there is a relatively narrow range of conditions such as temperature, skin moisture levels, and metabolic rate for which it can be said that most people experience thermal comfort. In general 4 physical variables influence thermal comfort. It is the air temperature, air velocity, relative humidity, and mean radiant temperature. There are also personal variables such as clothing insulation and activity level (metabolic rate). [8]

The thermal comfort discipline can be divided into three different approaches: psychological, physiological, and rational. The psychological approach uses the ASHRAE thermal comfort definition described above. In terms of simulation potential, this approach is not useful since the subjective opinions of individuals are used. On the other hand physiological approach considers signals obtained from thermoreceptors and the response of the thermoregulatory system, mediated through the hypothalamus. The physiological approach can also take into account the effect of acclimatization, that is the adaptation of the thermoreceptors to a different climate. Finally, the rational approach considers the thermal balance and physiological values of certain variables. In other words, the heat output must be equal to the heat input to achieve

thermal neutrality. At the same time, other physiological variables such as skin temperature or sweat production must be within certain limits. [8]

The rationale behind thermal comfort modeling is to optimize the environmental conditions in which humans work and live. From a purely economical standpoint maintaining optimal microclimatic conditions leads to higher efficiency. Furthermore, thermal comfort is the underlying factor in building energy consumption. Research into thermal comfort can bring overall energy consumption down. This is important because currently, buildings account for approximately 40% of the world's energy consumption. [8]

The nomenclature used for describing thermal models is not entirely consistent. Some literature describes thermophysiological models to be synonymous with thermal comfort models. Nevertheless, in different literature, it is any model that tries to predict the thermal state. In this work, the thermophysiological model will mean the thermal comfort model, with the main focus being on rational thermal comfort models.

1.5 Thermophysiological Models

Humans are exposed to a plethora of different thermal environments in their day-to-day lives. The potential to predict reactions of the human thermophysiological systems and the ability to adjust these environments to better suit human physiology has been the driving force in developing thermophysiological models, which are also known as thermal comfort models. Thermophysiological models aim to mathematical express and model physiological responses and heat transfer within the body and with the outer environment. The models may predict variables such as but not limited to skin temperature, core temperature, vasodilatation, vasoconstriction, and the amount of sweating.

In 1948 Pennes [9] postulated a mathematical model based on the temperature measured on the upper limbs of 9 participants. The modeled limb was assumed to be cylindrical and the rest of the body was not modeled. The equation proposed by Pennes has been widely accepted and is now known as the bioheat equation.

In the 1960s and 1970s, as computers became more powerful and numerical methods improved, thermophysiological models began to evolve and modeled the whole body. The first advanced model, from which a plethora of later models are derived, was developed by Stolwijk and dates back to 1971. A total of 25 nodes were used to represent the whole body. Stolwijk model was developed for NASA during the Apollo program to study the effect of extreme environments on the astronauts in space. [10], [11]

Since then many thermophysiological models have been developed most notably that of Tanabe [12], Fiala [1], and ThermoSEM [13]. The general direction is including more and more complexities and details of the human thermophysiological system and its interaction with the environment.

Despite significant advancements, wider utilization of thermophysiological models in predicting thermal responses is lacking. This is due to a lack of confidence in the predictive powers

of thermophysiological models. Thermophysiological models are frequently validated with experiments performed by authors of studies or a small set of experiments performed 40 or more years ago (Werner et al. [14], Stolwijk and Hardy [15], [16]). Ultimately a database of experiments against which all developed thermophysiological models could be validated is missing. [11]

1.5.1 Classification

Thermophysiological models can be categorized based on the number of segments or nodes used to represent the body, as can be seen in figure 2. In terms of segments, the body can be represented as having a single segment or it can be divided into multiple segments, each segment representing a part of the body (right arm, head, etc.). Single-segment can be either one-node, two-node, multi-node, or multi-element.

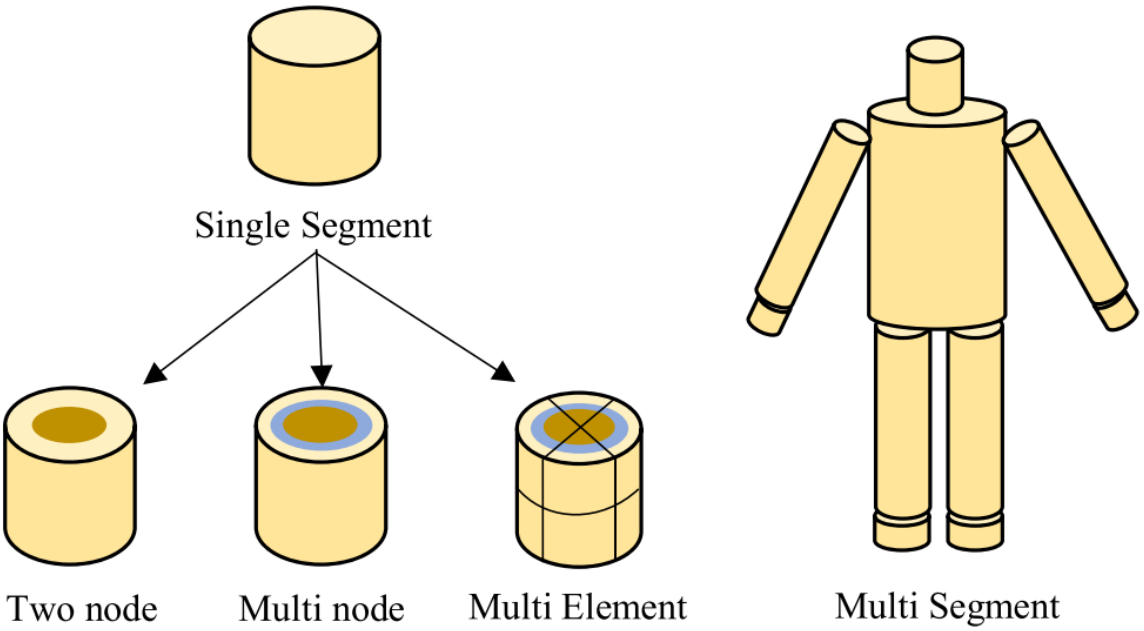

Figure 2: Classification of thermophysiological models. Modified from [17]

Single Segment Models

In single-segment models the body is a lumped object and does not contain many of the geometrical intricacies nor do they provide comprehensive thermal distribution. Single-segment models can be further subdivided based on the number of nodes into one-node or two-node models.

One-node models are a type of empirical model that treats the human body as a single, integrated entity exposed to the environment. Examples of these models include those developed

by Givoni and Goldman in 1971 for use in hot environments [18]. The body is generally modeled as a homogeneous cylinder and the thermoregulatory system is not explicitly included. These are the simplest models and due to the inaccuracies that modeling the body as a cylinder, disregarding different layers, etc. they are seldom used.

In **two-node models** the human body is divided into two concentric cylinders - shell node and core node, where the shell represents skin. The temperature in each node is considered uniform. Gagge's model, which was developed in 1971 and improved upon in 1986, is a well-known example of a two-node thermal model [19]. Heat transfer between these layers and between the shell and the core are included, along with thermoregulatory control functions.

Multi-Segment Models

Multi-segmented models were developed to address the limitations of single-segment models. Multi-segment models can be further subdivided into two-node, multi-node, or multi-element models.

The first **two-node** multi-segment model was developed in 1992 by Jones et al. [20] and was a modification to Gagge's single-segment two-node model from 1971 [19]. It contains the shell and core but further divides the body into sub-segments such as the head, torso, arms, and legs.

Multi-node models are more complex versions of the two-node models. The first and most influential multi-node model is the Stolwijk model [10]. Developed in 1971 it has 6 segments, where each segment has 4 nodes: core, fat, muscle, and skin node. With the central blood node, the model contains a total of 25 nodes. While this model does not contain equations for counter-current heat exchange or differences in local blood flow. Nevertheless building on these foundations several more detailed models such as that of Fiala [1], Tanabe (JOS) [21], or Berkeley[22].

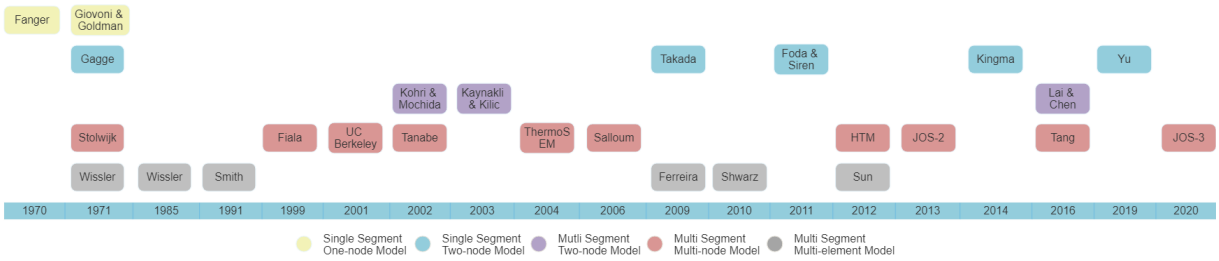

Figure 3: Timeline of developed thermophysiological models Modified from [17].

Multi-element models with multi-element models are the most complex and subsequently mostly developed in recent years. Unlike multi-node models, multi-element models simulate the human body as a multitude of body parts, without any subdivisions into nodes. Furthermore, multi-element models do not assume uniform node temperatures nor is the body necessarily idealized into spheres and cylinders, and can include complex geometric shapes. For example in 1985, Wissler [23] created a thermal model, which also includes mass balances for oxygen,

carbon dioxide, and lactic acid in ventilation. The model features a detailed passive system consisting of 15 elements connected by arteries, veins, and capillaries. Due to a limited computer capacity, the elements were assumed to be cylindrical. This does not apply and later models such as that of Sun et al. [24] or Tang [25] et al. include more geometric detail. Models can even include a full-scale voxel model of the human body even with internal organs. Nevertheless, as Kingma [13] pointed out more detail does not necessarily translate to more accurate outputs. This is because our understanding of the composition and regulation of local tissues is still incomplete. Furthermore, there is a trade-off between model complexity and simulation time, meaning that the more detailed and complex the model is, the longer it takes to run simulations.

1.5.2 Active System

Thermoregulation of the human body can be divided into two interacting systems: the active system and the passive system which is controlled by the active system. A schematic diagram of an active and passive system and their interaction can be seen in figure 4.

The active system maintains internal temperature within physiological bounds by controlling four regulatory responses: vasoconstriction, vasodilation, shivering, non-shivering thermogenesis, and sweating. The thermoregulatory system combines information from multiple thermal stimuli to be able to make an appropriate adjustment to keep the core temperature constant. The core temperature, mean skin temperature, and its rate of change are among the chief inputs for the active system. When there is excess heat vasodilation occurs. The amount of skin blood flow can go from almost non-existent (in limbs) during cold exposure, to a local 11 times increase from the basal value during heat exposure. If this is not enough vasodilation is accompanied by sweat excretion which helps the body cool down by evaporative cooling, increasing cooling power over 7-fold to the basal values. In cool conditions, blood vessels constrict. If this is not enough the body will start shivering and non-shivering thermogenesis. [1], [11]

Research has shown that the human body's ability to regulate its temperature is not controlled by a single input system, but rather by a complex network of inputs that work together to maintain balance. Various sites in the body are sensitive to changes in temperature, including the skin, brain stem, and deep tissue receptors.

1.5.3 Passive System

The passive system models the human body, heat transfer within the human body, and finally models heat transfer between the body and its environment. The interaction of the passive system with the active system can be seen in figure 4. The heat generated via various metabolic processes is transferred to other parts of the body mostly by blood circulation, the rest of the body effectively acts as a heat sink. One of the most important heat sinks is the biggest organ in the human body - the skin. Only a small amount of heat is transferred to the skin directly through conduction, most heat is transferred by blood using convection. To model heat transfer

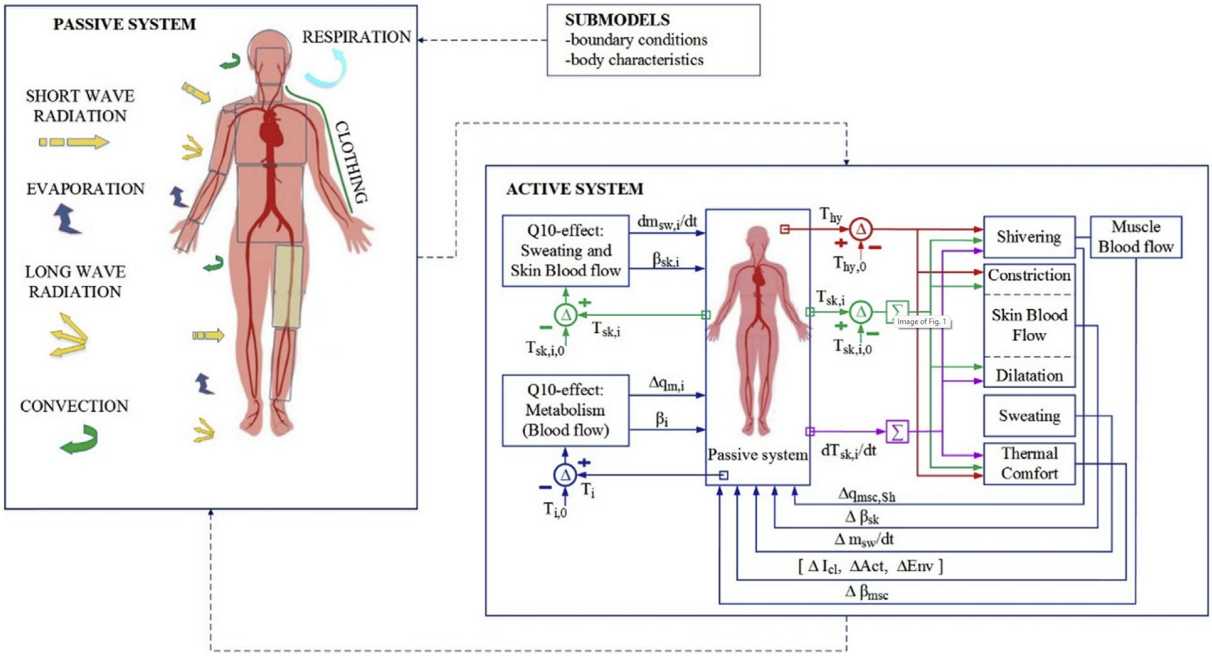

Figure 4: Passive and active system and their interaction [11]. Inputs of the active system are current skin and core temperatures, internal heat generation via metabolism, sweating, blood flow, etc. Based on the inputs the active system determines changes to the thermoregulatory responses which aid in reaching thermal comfort. Outputs of the active system are in a feedback loop and are also inputs of the active system.

inside a human body the thermal properties of tissues, such as bone, muscle, fat, and blood need to be considered. [26], [11]

Heat transfer between the body and its environment is mediated through a complex combination of thermal conduction, thermal convection, thermal radiation, and evaporation. Clothing also influences the exchange and should be taken into consideration. It has been estimated that at 20 °C in still air a resting nude person would lose about 60 % of the heat by radiation. The rest is lost through evaporation and convection, with only a very modest loss through conduction. [26]

1.5.4 Pennes Bioheat Equation

Pennes Bioheat equation is a mathematical description of the heat transfer in biological tissues. It was first developed by C. K. Pennes in 1948 [9] and has since been widely used with minor adjustments in various fields, such as biomedical engineering, thermoregulation, and hyperthermia treatment. The bioheat equation is widely used by thermophysiological models, such as that of Fiala [1], ThermoSEM [13], or Berkeley [22]. As such it has been pivotal to the development of thermophysiological models and will be described below.

The Pennes Bioheat equation is based on the principle of conservation of energy and describes the balance of heat transfer in tissue with blood perfusion. It takes into account the thermal properties of the tissue, the blood flow rate, and metabolic heat production. The equa-

tion can be written for cylindrical coordinates as follows:

$$\rho_t c_t \frac{\partial T_t(r,t)}{\partial t} = k_t r \frac{\partial}{\partial r}\left(r \frac{\partial T_t(r,t)}{\partial r}\right) + \omega_b \rho_b c_b (T_{a0} - T_t(r,t)) + Q_m \quad (1)$$

Where:

ρ_t = is the tissue density

c_t = is the tissue-specific heat

$T_t(r,t)$ = is the tissue temperature as a function of radial position r and time t

t = is time

k_t = is the tissue thermal conductivity

ω_b = is the blood perfusion rate per unit volume of tissue

ρ_b = is the blood density

c_b = is the specific heat of blood

T_{a0} = is the arterial blood temperature

Q_m = is the metabolic heat production rate per unit volume.

There are a few inaccuracies in the Pennes model which arise from the following assumptions: prevenule and prearteriole heat transfers are not considered, the blood flow direction is not accounted for, and capillary beds receive blood at core temperature. [1]

1.6 Examples of Thermophysiological Models

This section describes recently developed thermophysiological models that are selected to be most applicable to the thermal data collected for this thesis. Selected models include the Fiala model, ThermoSEM, Berkeley, and JOS-3. Model JOS-3 will not be described here as it is described in detail in chapter 2.

1.6.1 Fiala

The first version of the Fiala multi-node thermophysiological model dates back to 1998 [1]. Since then Fiala model was incorporated with some modifications into several commercial software such as Thesus-FE or Rad-Therm. The passive system comprises an average man who weighs 73.5 kg and with a surface area of 1.86 m^2. The human body is divided into 10 segments with the head having a spherical symmetry and the rest of the segments having cylindrical symmetry.

All segments of the passive system are made up of concentric layers of tissues. The model distinguishes seven types of tissue (brain, lung, bone, muscle, adipose, skin, and internal organs), which differ in their physical properties. Each tissue layer is further divided into three

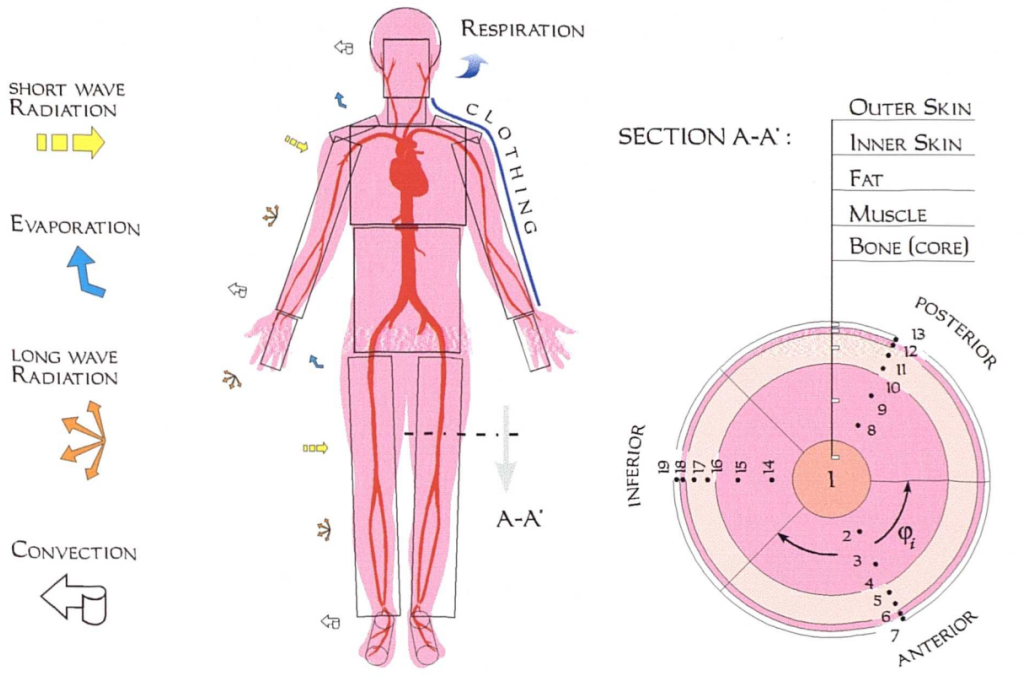

Figure 5: A schematic diagram of the Fiala's passive system [1]. Each segment is split into three sectors, each containing a set of tissues described in section A-A'.

sectors that have the shape of a sector of a circle. The reason behind this division is that there might be asymmetry in the heat dissipation, for example, due to the differences in mean radiant temperature. This can happen for example if the inner thighs are touching each other during sitting. The heat transfer between the tissues is calculated by Pennes bioheat equation described in equation 1.

The active system comprises four mechanisms that maintain a constant temperature in the body. These include vasodilation, vasoconstriction, shivering thermogenesis, and sweating. The methodology used for finding out the regulatory responses of the central nervous system is obtained from doing regression analysis on data obtained from experiments. Several experiments from literature covering cold, neutral, and hot conditions were used for these purposes. Both steady state and transient conditions were considered. The responses of the thermoregulation system that were observed during experiments were applied to the passive system. Then multi-linear regression was used to obtain the resulting control equations of the active system. The validation was done with core and skin temperatures and with thermoregulatory responses and they were shown to be well correlated with the experiments.

Further study by Martínez et al. [27] has shown acceptable precision for core (RMSD 0.26 °C) and mean skin temperature (RMSD 0.92 °C). Furthermore, the study has shown an average RMSD of 1.32 °C for local skin temperatures.

1.6.2 Berkeley Comfort Model

Berkeley Comfort Model is based on Stolwijk's 25-node thermophysiological model and Tanabe's work. It has been developed in the year 2001 and includes several improvements over the Stolwijk model. Most notably even though the model was developed using 16 segments the body can be segmented into an arbitrary amount of body segments [22]. This allows more accurate simulation of asymmetric and transient phenomena compared to set node models. Such as local variations in temperatures or heat flux. An example simulation might be a person sitting near the window with the sun shining only on certain body parts while being close to an air-conditioning. Each segment is made of 5 layers, that is core, muscle, fat, skin, and clothing. Clothing includes moisture and heat capacitance.

Further improvements compared to Stolwijk include the addition of countercurrent heat exchange, thermoregulation responses (vasoconstriction and vasodilatation, sweating) are now explicitly modeled, and physiological variations. Physiological variation interpersonal differences such as height or BMI (body mass index). Despite the number and influence of interpersonal differences most early thermophysiological models do not take them into consideration. Authors of this model have developed a "body builder" model that takes into account six key characteristics of a person's body - height, weight, age, gender, skin color, and body fat - and maps them to physiological data used by the comfort model. For example, the study found that outputs of the model when body fat percentage is increased from 14 to 28 % can cause a skin temperature change of roughly 1 °C.

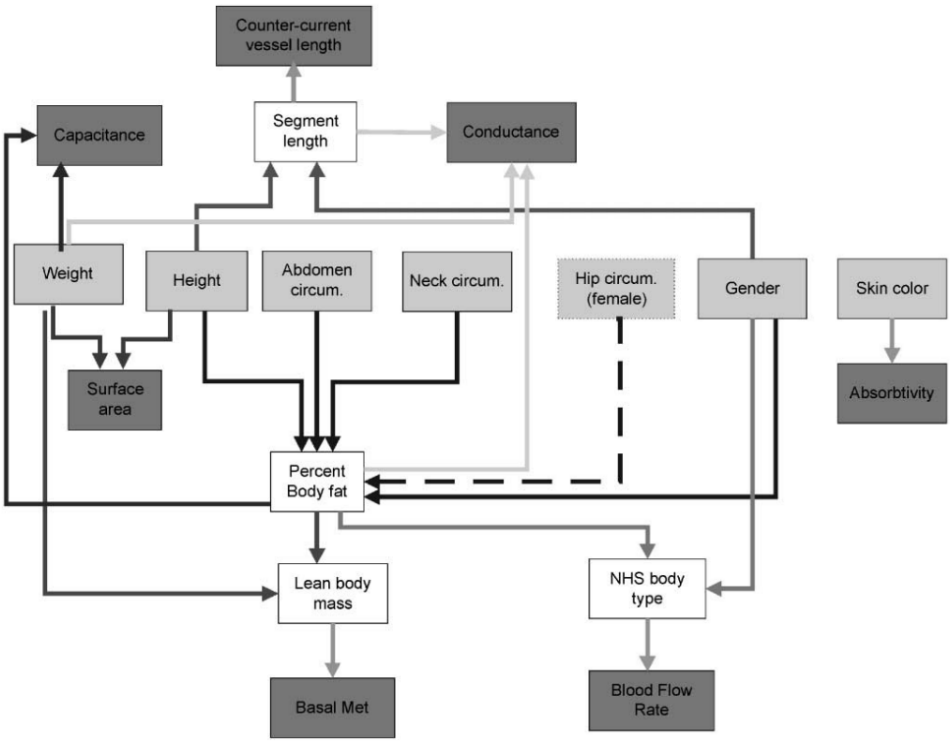

Figure 6: Flowchart of the Berkeley body builder model [28]. Light grey sections are the inputs for the model. Dark grey sections are the calculated outputs used by the Berkeley model.

The model has been validated for steady-state conditions, transient conditions, and non-uniform environments. More notably cold-exposure transients and hot-exposure transients validation were performed. Most skin temperatures simulation were within 1 °C while core temperatures were within 0.5 °C. [22]

Interestingly the equations used for the model development are not included in the study. The model has been created using the C++ programming language, and it follows an object-oriented approach. Not allowing third-person parties modification of the underlying software, it is distributed as an executable file. [22]

1.6.3 ThermoSEM

Thermophysiological Simulation Model Eindhoven Maastricht (ThermoSEM) was developed by Kingmaet al. in 2014 [13] It is based on Fiala's model, which was an improvement on Stolwijks' multi-segmental thermoregulation model. ThermoSEM differs slightly from Fiala's model in that it splits the arms and legs into upper and lower parts and corrects skin perfusion for tissue volume. However, the main difference between the two models is in the active part of ThermoSEM. The active part aims to increase the accuracy of the active part by incorporating neurophysiological concepts for thermoregulation.

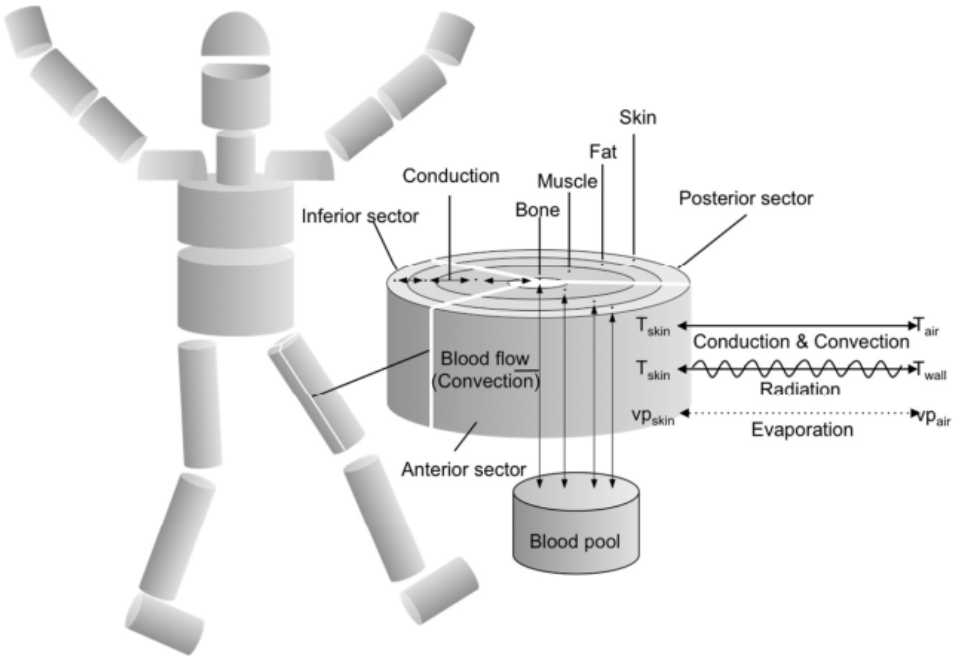

Figure 7: Passive system of ThermoSEM [13].

The passive system comprises 19 segments as can be seen in 7. Segments are comprised of concentric cylinders and concentric spheres. Each segment is composed of 5 layers (bone, muscle, fat, inner skin, and outer skin). There is a slight difference in the passive system compared to the Fiala model, mainly the subdivision of extremities into upper and lower parts

and the correction of skin perfusion for tissue volume. Furthermore, each segment is divided into three sections (anterior, posterior, inferior) which define the orientation of the segment. This allows for the consideration of asymmetric boundary conditions. Pennes' bioheat equation is used to model convection and conduction within the body while boundary heat transfer is modeled according to Fiala et al. [1].

The active system is also based on Fiala but incorporates thermal reception data and neural pathways involved in skin blood flow control during thermoregulation. It aims to improve simulation accuracy since when in a thermoneutral environment the skin blood flow is the only mechanism used to regulate the body temperature. The thermoregulatory system is modeled in 5 steps as can be seen in figure 8. First, the fire rates from cold and warm sensitive neurons are collected. Second, the neuron fire rates are integrated at neurons located in the spine. Third, the spinal column neurons are projected to the medial pre-optic in the hypothalamus where they excite or inhibit warm sensitive neurons. Fourth, the neurons in the hypothalamus inhibit neurons in the ventromedial medulla and its associated weights. Fifth, ventromedial medulla efferent neurons control skin blood flow.

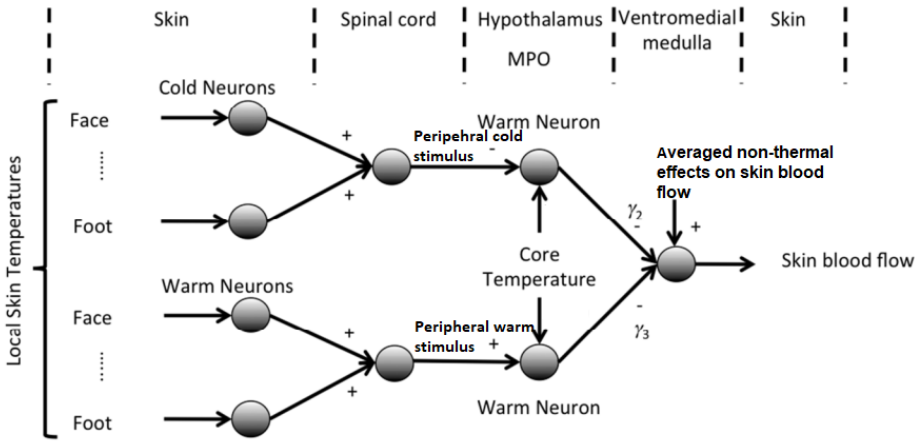

Figure 8: Neuronal pathways involved in the control of skin blood flow in ThermoSEM [13].

ThermoSEM has been validated for mild temperatures in the range of 20 to 35 °C. In terms of environmental conditions, it has been validated for transient and non-uniform conditions. Individual characteristics such as height and weight can be taken into account into account.

1.7 Applications of Thermophysiological Models

As the thermophysiological models get more complex and accurate many fields recognize the importance of thermal modeling. They are particularly useful in evaluating thermal comfort and heat stress, as well as designing and developing environmental control in complex thermal environments. Examples of complex thermal environments include but are not limited to spaceflight, airplanes, and the automotive industry. Thermophysiological models have also been used in

the medical field i.e. to predict patient temperature during cardiac surgery.

1.7.1 The Universal Thermal Climate Index

The Universal Thermal Climate Index (UTCI) is an international index that aims to assess thermophysiological responses across a broad range of outdoor thermal conditions. Through collaboration between leading experts in areas such as thermophysiology, metrology, and climatology the UTCI was established in 2009. The UTCI calculates equivalent temperatures using a thermophysiological model that takes into account wind, mean radiation temperature, humidity, and air temperature. As such it can be used by public weather services, public health agencies, and urban planning. It can also be used in tourism and recreation settings to inform decisions about outdoor activities and events, and in climate impact research to better understand the effects of changing thermal conditions on human health and well-being. [11]

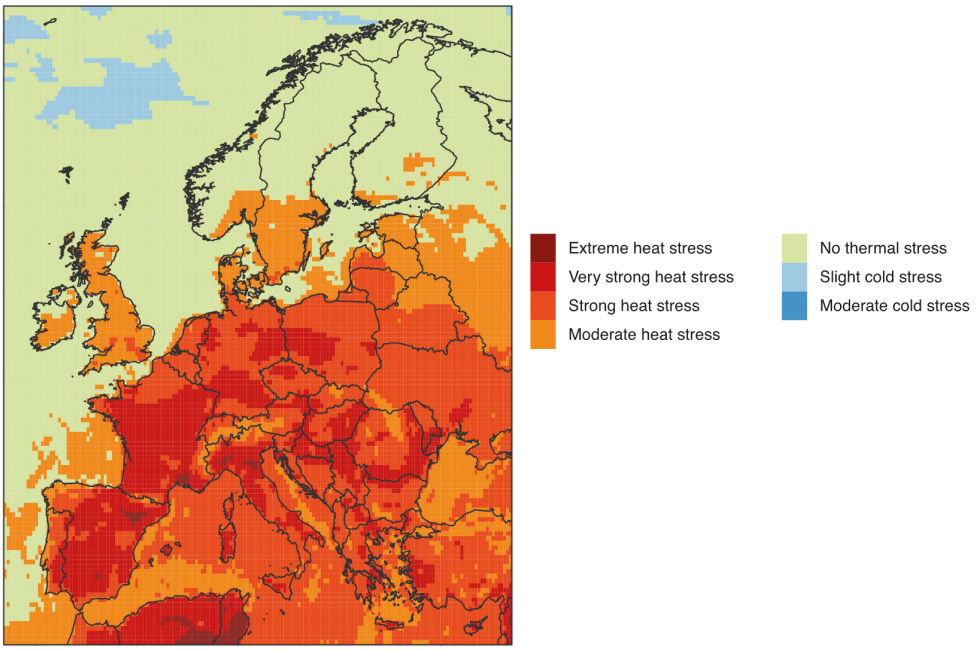

Figure 9: Distribution of heat stress evaluated with UTCI during the June 2019 heatwave in Europe [29].

As the knowledge in the field of thermophysiological models progressed experts have agreed that UTCI should include the complete human heat budget and thermal response of an average human. As a part of the COST Action 730 initiative wide range of thermophysiological models were considered and in the end, the Fiala model was chosen. For the purposes of UTCI, the Fiala model was expanded and evaluated producing a UTCI-Fiala model. Along with some other minor changes the new model includes an adaptive clothing model, which takes into consideration behavioral adjustments of clothing insulation, the effect of wind, and clothing's permeability. After providing good performance in a large-scale validation study the UTCI-Fiala model was incorporated into UTCI. [30]

1.7.2 Automotive & Airplanes

Cars, buses, and airplane cabins have environmental conditions that are not uniform and generally require individuals to spend extended periods inside them. Therefore it is important to design them for thermal comfort. The Fiala model was expanded on and implemented inside a commercially available THESEUS-FE software, to simulate complex environments inside various types of transports and to simulate the thermal comfort of passengers. The thermophysiological model is used in conjunction with a detailed model of the vehicle cabin is used during the vehicle development phase. Audi, BMW, and Renault are just a few examples of car manufacturers that use THESEUS-FE. [31]

1.7.3 Spaceflight

The first use of thermophysiological models dates back to 1971 when Stolwijk thermophysiological model was developed specifically for the National Aeronautics and Space Administration (NASA) [10]. It has been followed by a 41 Node Man model 4 years later [32], which was developed in FORTRAN language. NASA has used human thermal models to design and develop environmental control and life support systems. Nevertheless, the development of space suits for extended extravehicular activities also has a unique need for thermophysiological models. Space suits can be exposed to various extreme conditions, such as extremely cold temperatures or quite high asymmetrical thermal radiation coming from the sun.

1.8 Aims & Contributions

The thesis was done in cooperation with a scientific team from Masaryk University, which is developing and validating a new method for stress measurement based on a calculation of stress entropy load [33]. Thermophysiological models may serve to simulate thermal responses vital to the calculation of stress entropy when thermal data may not be available.

Thus, the thesis is focused on the selection of a suitable model for the use case scenario of Antarctica and the validation of its use for the thermal data obtained during the experiment. The objectives of the thesis are: 1) to compare and select thermophysiological models for the use case scenario of Antarctica, 2) to collect/pre-process data from the Antarctica mission by Masaryk University, 3) to apply the selected thermophysiological model to given conditions, 4) to compare the outputs of the selected model with Antarctica data and evaluate the utility of the model.

> Specific question 1: What is a suitable thermophysiological model for the use case scenario of Antarctica?
>
> Specific question 2: How well does the selected model compare in terms of accuracy to data collected by Masaryk University's Antarctica mission?

2 Materials & Methods

The first part of the materials & methods chapter discusses the benefits and disadvantages of selected thermophysiological models and selecting the most suitable model for the use case of this thesis. The model is then described in detail. The second part describes the experiment in Antarctica. The third part focuses on pre-processing and choosing input values for the selected model.

2.1 Thermophysiological Models Comparison and Selection

In the following text selected thermophysiological models will be compared. Next conditions of the experiment in Antarctica will be analyzed and a suitable model will be selected.

A comparison of selected models can be found in table 1. Multi-element models were considered as well but were ultimately disregarded, even though these models are the most complex and reflect the geometric complexities of the body more accurately. As Kingma [13] pointed out complexity does not necessarily translate to more accurate outputs. This is because the scientific understanding of the thermal regulation of local tissues is still incomplete. Ultimately the evidence that multi-element models are more accurate is absent.

To ensure the accuracy of the models, simulation results are compared with experimental data. Selection of the model should include model accuracy for thermal conditions in which the experiment took place and compare it against the accuracy of other models. There have been some studies comparing the accuracy of their developed model with one or two others. An overview of available comparison studies can be found in Katic et al. [11]. However, these include only a few models and a larger comparison of the accuracy of different models with the same thermal conditions and other conditions being equal is not available. This may be due to the unavailability of the models, which makes it necessary to rely on figures in published research, or due to the inaccessibility of the experiment data. Creating a database with a variety of thermal, physiological, and other conditions while publishing the model accuracy could help bridge the gap.

Even though a comprehensive comparison is not available, the validation tests often include that of Stolwijk and Hardy from 1966 [16], [15] for transient conditions and Werner et. al from 1980 [14] for steady-state conditions. The experiment by Stolwijk and Hardy had participants spend 60 minutes at a thermoneutral temperature of 28 °C then quickly transfer to an environment with 33, 38, 43 or 48 °C for 120 minutes then finally they were transferred back to previous

Table 1: Comparison of main characteristics and properties of thermophysiological models.

Model	Passive system	Active system based on	Physiological characteristics	Environmental conditions
JOS-3	- 17 segments - 85 nodes - Core, muscle,fat and skin	Stolwijk	Height, weight, age, gender, body fat	- Steady-state - Transient - Non-uniform
Berkeley Comfort	- Arbitrary amount of nodes - Core, muscle, fat, skin, clothing	Stolwijk	Height, weight, age, gender, skin color, body fat	- Transient - Non-uniform
ThermoSEM 2014	- 19 segments - Bone, muscle, fat, inner skin, outer skin - Spatial sectors: anterior, posterior, interior	Fiala but with neurophysiology concepts	Average person	- Transient - Non-uniform
Fiala	- 15 segments - 187 nodes - Spatial sectors: anterior, posterior, interior - Brain, lung, bone, muscle, fat, skin, viscera	Regression	Average person	- Steady-state - Transient - Non-uniform

conditions of 28 °C for another 60 minutes. A similar experiment was done for cold exposure transients as well. An experiment by Werner et al. [14] had participants spend 60 minutes at 30 °C and then move to an environment with air temperature set at 10, 20, 30, 35, 40, 45, or 50 °C for 120 minutes.

Table 2: Comparison of model accuracy under the same environmental conditions.

Model	Validation	Steady-state accuracy	Transient accuracy
JOS-3	Steady-state: Werner et al. Transient: Stolwijk and Hardy	RMSD 0.50–1.77 ℃, higher temperatures had highest deviation	RMSD 0.58–0.83 ℃
Berkeley Comfort	Steady-state: Werner et al. Transient: Stolwijk and Hardy	Deviation within 1 ℃ for most segments	Figure
ThermoSEM 2014	Conducted own experiments	N/A	N/A
Fiala	Transient: Stolwijk and Hardy	N/A	RMSD 0.30–0.78 ℃

As can be seen in table 2 JOS-3 and Fiala share a validation test for transients conditions in common. Both models have comparable mean skin temperature RMSD values. The experiments have each a sample size of 3 for cold exposure transients and hot exposure transients. The age is between 22-25 years old. All participants are males. Thus mode by Fiala has a slight advantage since the individual's characteristics are close to the average man, if that would not be the case the deviations would probably be bigger. JOS-3 and Berkeley model share the experiment by Werner in common. Berkeley model [22] regrettably does not share RMSD but instead states: "For most segments, the skin temperature simulation is within 1 °C." The Berkeley model was also validated by Stolwijk and Hardy but selected only some step changes making it hard to meaningfully compare.

Selection

The experiment was done in a room without temperature control. Ambient temperature data collected show the air temperature range to be between 20 to 30 °C. The temperature trend goes from lower air temperatures to higher, which is in agreement with conditions during measurement since the heating was turned to a higher setting so the participants would not feel cold. Therefore the selected model has to be validated in transient conditions. It can be reasonably assumed that the conditions were uniform and symmetrical and no part of the body was exposed more to conditions such as sun, AC, or central heating.

During the experiment, several physiological characteristics were obtained. These include age, height, weight, and gender. Ideally, all of these should be used to increase the accuracy of the model. Body fat percentage was not measured. Next, the skin temperature sensor placement covers the whole body. These should correspond to how the body was divided in the passive system of the models. This is of course not entirely possible since usually only one part of a limb was measured, this is deemed acceptable by ISO 9886 [34], and measurement on the other part should be symmetrical.

All of the temperature sensors and humidity sensors used in the experiment had a measuring frequency of 2 Hz. In the models, there is frequently a minimum simulation time-step. This is reasonable when modeling in steady state conditions or even transient conditions measured on a relatively long time frame (30+ minutes). Nevertheless, as the measurement time of a single measurement is usually between 10 to 20 minutes and ambient temperature can change by several degrees during that time, models allowing time steps in seconds will be chosen.

Although the model by Fiala is one of the most adopted models and complies with the requirements defined above a detriment is that individual physiological characteristics are not considered. The ThermoSEM model was based on the original Fiala model which used an average man so it does not consider physiological characteristics.

Berkeley model according to the 2001 study by Huizenga et al. [22] has dedicated software. Nonetheless, it is not publicly accessible. Even studies comparing the Berkeley model [35] to others only compared outputs of the model based on the figures published by Huizenga et al. Equations that would permit the model to be programmed also have not been made public. Furthermore, the minimum simulation time step is 1 minute.

In conclusion, the JOS-3 model has been validated with comparable accuracy to other models it was compared to and in the required environmental conditions. Its open architecture enables possible modifications, the simulation time step is variable and physiological characteristics can be taken into account. The passive system segmentation is fully covered by the temperature sensor locations used in this experiment and defined in ISO 9886 [34]. Therefore it was chosen to be the most suitable model for the collected data.

2.2 JOS3

Based on the Stolwijk model [16] Tanabe et. al. [21] developed a 65-node thermoregulation model in 2002 which came to be known as the JOS-1 model. JOS-1 is used to predict the body's temperature response to various environmental conditions, including air temperature, relative humidity, and clothing insulation. The model takes into account the heat production by the body, heat loss to the environment, and the balance between these two factors to estimate the core and skin temperature of the body. Parts of the original team continued to make improvements to the original model, producing JOS-2 in 2013 and JOS-3 in 2020. The previous version will be briefly described in the following paragraphs.

In **JOS-1** the body is divided into 16 segments (head, chest, right arm, left arm, etc.). Each segment contains the core, muscle, fat, and skin layer. Furthermore, there is a central blood node in which all 4 segments exchange heat, basically modeling the blood flow. This segment is the 65th node. Heat is transferred through the 4 layers via conduction. The effective radiation area was established for 3 postures, i.e. lying, standing, and sitting. [21]

JOS-2 is a revised version of the JOS-1 model. It added a detailed vascular system. Furthermore, differences in sex and age were considered. The entire body is divided into idealized 17 segments with a shape of either a sphere (head) or a cylinder (rest of the body). All segments now in addition have an artery blood pool and a vein blood pool. Furthermore, the effects of arteriovenous anastomoses (AVA) and superficial veins in the limbs have been taken into consideration. [36]

JOS-3 included the effects of brown adipose tissue, aging, and thermal radiation gain from the environment. Furthermore, equations for calculating shivering thermogenesis, basal metabolic rate, and sweating distribution have been modified. Many of the limitations of the previous version have been greatly improved in this update. The model's accuracy has been tested against measurements taken from human subjects, and it is more accurate in predicting heat production in both young and older subjects, as well as mean skin temperature in older subjects, particularly in cold environmental conditions. The concept of JOS-3 can be seen in figure 10. Furthermore, it adopted open source code philosophy making the model quickly adaptable and modifiable. [12]

2.2.1 Body construction

JOS-3 comprises 85 nodes, which include: 17 skin nodes, 17 artery nodes, 17 vein nodes, 17 core nodes, 12 superficial vein nodes and 2 muscle nodes, and 2 fat nodes. All of these nodes including the segmentation of the body to 17 segments can be seen in figure 10. In general, JOS-3 has four layers (core, muscle, fat, skin), although not all of the segments have all layers. The layer names are always the same even though some segments may not contain much of a muscle or fat layer such as the head. Instead, it can be thought of as thermal layers 2 and 3, but JOS-3 maintains the terminology for layers defined above to stay consistent.

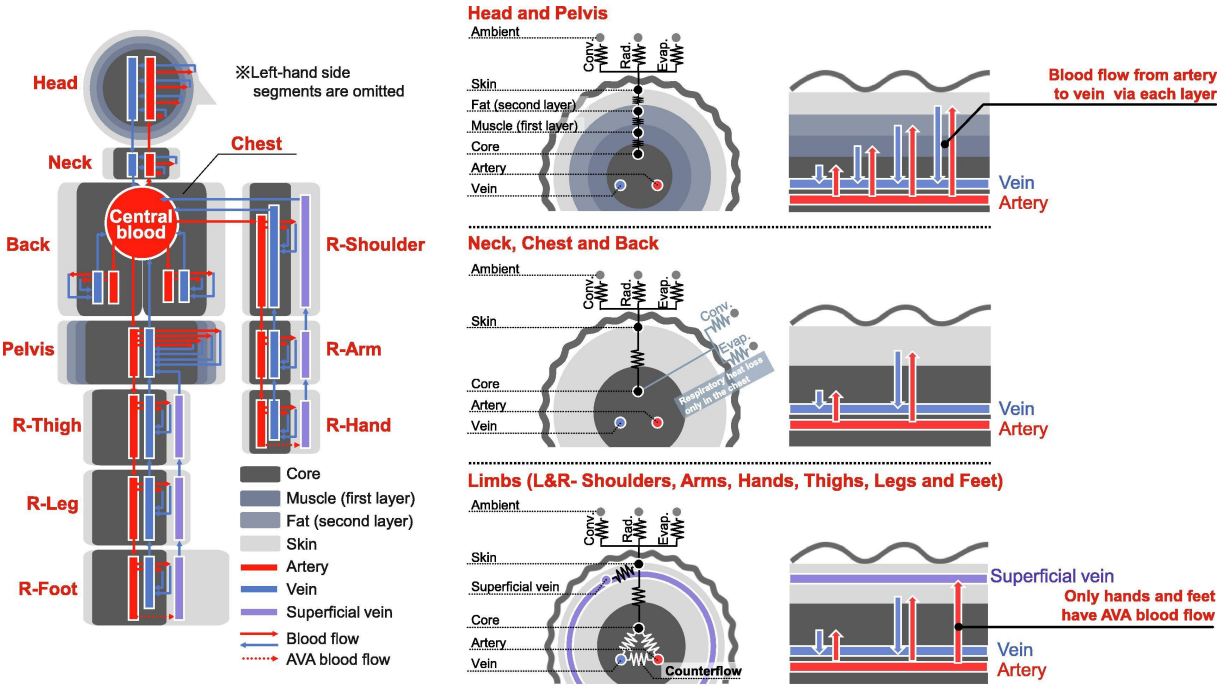

Figure 10: Conceptual depiction of JOS-3 [12].

The head has various nodes including arteries, veins, cores, muscles, fat, and skin. Meanwhile, the neck, chest, and back segments have similar nodes except for the muscle and fat nodes. Limb segments also have their own set of nodes which includes the superficial vein. Blood pools for arteries and veins are situated at the core layer, while the superficial vein pool is found in the middle skin layer. The hand or foot segment has arteriovenous anastomosis (AVA) blood flow, which connects the artery to the superficial vein pool. Furthermore, the model assumes that blood from multiple upstream paths is fully mixed before flowing downstream. [12]

2.2.2 Passive system

The passive system comprises the model of the body mentioned previously, equations governing the complex heat exchange occurring inside the body, and the boundary conditions which model heat exchange between the environment and the simulated body. Each node has a variant of the heat exchange equation which is described below. For simplicity, it has been summarized and in reality, some of its parts are zero for some nodes. Parts of the heat balance equation will be described below. For a more comprehensive overview, coefficient values and a complete set of heat balance equations for each type of node see [12].

$$C\frac{dT}{dt} = Q + B + D - RES - E - C - R + SW \tag{2}$$

where C is the heat capacity of the considered node, and T is its temperature. Q is the heat production of the node, B is the heat exchange by blood, D accounts for heat exchange between layers in the same node, RES is heat loss by respiration (only in the chest), E (evaporation) is

the latent heat loss from the skin, C and R is the convective and radiant heat loss, finally SW represents heat gain from short-wave radiation.

Heat production of a single node is calculated as a sum o heat produced by basal metabolic rate M_{base}, external work M_{work}, shivering thermogenesis M_{shiv} and non-shivering thermogenesis M_{nst}.

$$Q = M_{base} + M_{work} + M_{shiv} + M_{nst} \tag{3}$$

Heat generation by external work, shivering, and non-shivering thermogenesis occur in the core layer of each segment except for the head, where the originating layer is the muscle layer. Shivering and non-shivering thermogenesis is controlled by the active system.

Sensible heat loss to the environment comprises convective heat loss C and radiant heat loss R. For a single skin node, it can be calculated as shown in equation 4 and 5.

$$C + R = h_t.(T_{sk} - T_o).BSA \tag{4}$$

$$\frac{1}{h_t} = 0.155.I_{cl} + \frac{1}{f_{cl}.(h_c + h_r)} \tag{5}$$

where h_t is total heat transfer coefficient, T_{sk} node skin temperature, T_o operative temperature and BSA is body surface area. For the second equation, I_{cl} is clothing insulation of the node, f_{cl} is clothing area factor, h_c, and h_r are radiative and convective heat transfer coefficients which were obtained via thermal manikin experiments.

Heat loss by respiration is comprised of latent (evaporation) heat loss and latent respiration heat loss as a function of the total heat produced by the body and is calculated by equation 6. The first term on the right side is the latent heat loss and is dependent on ambient air temperature $T_{a[0]}$. Compared to latent heat loss its effect is relatively small. The second term on the right side is the latent heat loss and is dependent on the water vapor pressure of the ambient air $p_{a[0]}$.

$$\begin{aligned} RES = &\left\{0.0014 \cdot \left(34 - T_{a[0]}\right) + 0.0173 \cdot \left(5.87 - p_{a[0]}\right)\right\} \\ &\cdot \sum_{i=0}^{16} \left(Q_{cr[i]} + Q_{ms[i]} + Q_{fat[i]} + Q_{sk[i]}\right) \end{aligned} \tag{6}$$

2.2.3 Active system

The active system entails thermoregulation mechanisms of the body which are aiming to reach thermal equilibrium with the environment also known as the thermoneutral zone, which is defined through setpoint temperatures. Specific parts of the active system are described below. For a more comprehensive overview and specific values of mentioned coefficients see [12].

Thermoregulation mechanisms include vasodilatation, vasoconstriction, perspiration, shivering, and non-shivering thermogenesis and are conceptualized as thermoregulation signals. The

rate of thermoregulation is calculated from an error signal

$$Err_{j[i]} = T_{j[i]} - T_{setp,j[i]} \tag{7}$$

where $T_{j[i]}$ is the actual layer temperature and $T_{setp,j[i]}$ is the setpoint temperature of the layer. The setpoint temperature according to Takahashi et al. [12] is defined as "the body temperature of the model that does not have a thermoregulation system (only a passive system) under thermal neutral operative temperature, based on the PMV-model (relative humidity = 50%, air velocity = 0.10 m/s, PAR = 1.25, and whole clothing insulation = 0.0 clo)."

Based on whether the $Err_{j[i]}$ is positive or negative it is determined whether the cold receptor or warm receptor is activated, the other will always be zero. The integrated error signal in the warm or cold receptor is calculated by equation 8 and 9 respectively.

$$Wrms = \Sigma_{i=0}^{16} SKINR_{[i]}.Wrm_{[i]} \tag{8}$$

$$Clds = \Sigma_{i=0}^{16} SKINR_{[i]}.Cld_{[i]} \tag{9}$$

The $SKINR_{[i]}$ is the distribution coefficient of thermal receptors. The skin blood flow is determined by previously established error signals and is expressed in equation 10. The vasodilatation signal DILAT and vasoconstriction signal STRIC are expressed in equation 11 and 12 respectively.

$$BF_{sk[i]} = \frac{1 + SKIND_{[i]}.AGdilat_{[i]}.DILAT}{1 + SKINC_{[i]}.AGstric_{[i]}.STRIC}.BFB_{sk[i]}.2^{\frac{Err_{sk[i]}}{6}} \tag{10}$$

Where $SKIND_{[i]}$, $SKINC_{[i]}$ is node distribution coefficient of vasodilation and vasoconstriction respectively. $AGdilat_{[i]}$, $AGstric_{[i]}$ is the aging effect on vasodilation and vasoconstriction. The vasomotion response worsens with age. $BFB_{[i]}$ is the node basal blood flow rate.

$$DILAT = 100.5 \cdot \mathrm{Err}_{cr[0]} + 6.4 \cdot (WRMS - CLDS) \tag{11}$$

$$STRIC = -10.8 \cdot Err_{cr[0]} - 10.8 \cdot (WRMS - CLDS) \tag{12}$$

In conclusion, the active system of JOS-3 behaves like a closed-loop feedback system with a negative feedback loop. On the input, there is a difference between the actual temperature (cold and warm sensors) and the reference setpoint value. The thermoregulatory mechanisms react proportionally to the difference.

2.2.4 Validation

The JOS-3 model was validated in three experiments which were conducted by Stolwijk and Hardy [16][15], Werner et al. [14] and Inoue et al. [37]. which tested performance in transient

conditions, steady-state conditions an aging effects respectively. First, two experiment designs were briefly described in section 2.1. In addition to these tests, JOS-2 validation included a car cabin test for transient conditions.

The experiment by Inoue et al. consisted of 9 younger (20-25 years) men with 10 older (60-71 years) men who were studied in two cold environments. Participants were instructed to be dressed only in swimming trunks and spend 60 minutes sitting in 28 °C. They were then asked to move to another chamber for 60 minutes where the air temperature was either 12 or 17 °C. The mean skin temperature RMSD for the older group was 0.2 and 0.17 for 12 and 17 °C respectively. For the younger group, The mean skin temperature RMSD was 0.61 and 0.27 for 12 and 17 °C respectively. [12]

2.2.5 Limitations

Although the model is not limited to any specific ethnicity, it may need to adjust the proportions of body tissues to obtain more accurate results. These can vary slightly depending on the ethnic group. Another limitation of JOS-3 is that it does not consider hot acclimatization, which may increase sweating efficiency, lower core temperature, and heart rate, and increase skin blood flow for identical core temperatures. Thus it may not accurately model inhabitants in hot climates, such as Southeast Asia. [12]

Lastly, the clothing layer represents clothing only in terms of thermal resistance, meaning it does not take into account heat capacity, moisture absorption, or release properties of clothing. This can have a negative effect on the accuracy when heavy clothing is worn which has high clothing insulation values. Furthermore, this can have a negative effect where the pumping effect occurs (movement of air or moisture in and out of the clothing layers as a result of body movement). [12]

2.3 Experiment design

Data were obtained during a longitudinal study on the trajectory of stress, taking place at the Johann Gregor Mendel Czech Antarctic station located at James Ross Island. A team member different from the author of this thesis was tasked with collecting the data. The expedition started on 16th of December 2021 and ended on 8th of March 2022. It also included a compulsory 10-day Covid-19 quarantine in Chile from the 18th of December.

The study collected data for this thesis but at the same time collected a plethora of other measurements relating to stress. Other variables which were measured include electrocardiogram, respiration flow, and carbon dioxide levels during exhalation and inhalation. These measurements can then be used to calculate cumulative specific entropy and ultimately stress entropic load. Calculation of stress entropic load is not the goal of the thesis but for those interested the process is outlined in a study by Zlámal et al. from 2018 [33]. The experiment, therefore, contains tasks such as orthostatic tests, the Iowa Gambling test, and Psychomotor Vigilance Task,

which are designed to put organisms under pressure and possibly induce a stress response in the participants.

2.3.1 Participants

The research project received approval from the ethics board of Masaryk University and all participants provided informed consent. The study involved 16 participants, 11 males, and 5 females. Half of the participants had previous expedition experience, while the other half were attending for the first time. While the majority (12) of the participants were from the Czech Republic, one was British and three people were from Slovakia but resided and have been working in the Czech Republic. Further basic physiological information about the participants can be found in table 3.

Table 3: Physiological characteristics of the participants.

Variable	Baseline characteristics (n = 16)
Age	35.4 ± 10.5
Height	176.3 ± 10.7
Weight	73.6 ± 15.9

While staying at the Antarctic station, participants stayed in a room with 1 to 2 other people. Due to geographical remoteness and therefore lack of usual infrastructure, there was no internet connection. Although participants were allotted 10 minutes for the use of satellite phones every day for their personal needs. These conditions were standard for the station and were not part of the experiment.

2.3.2 Instrumentation

Measurement devices were mounted on a vest along with a control unit. The control unit collected data from airflow sensors on the mask, pneumotachograph belt, ambient air humidity sensors, ambient air temperature, ambient pressure, CO_2 and O_2 sensors, ECG sensors. The control unit communicated wirelessly with the software located on a laptop. Sensors for CO_2 and O_2 were connected to a mask that covered both the mouth and nose. An example of the instrumentation mounted on the body can be seen in figure 11.

Furthermore, 14 wireless infrared temperature sensors were part of the setup. They were placed on the skin via a sticky kinesio-tape. The exact type of thermometer used is MLX90614ESF-DCA-000-SP.

Table 4: Logging frequency and type of sensors relevant to the study.

Sensor	Frequency [Hz]	Type of sensor	Accuracy
Skin temperature	2	MLX90614ESF-DCA-000-SP	±0.5 °C
Ambient air temperature	2	SHT35	± 0.1°C
Ambient air humidity	2	SHT35	± 1.5 %
Ambient air pressure	2	BMP388	± 0.5 hPa

Figure 11: Measurement instrumentation on a person.

2.3.3 Procedure

The measurements were carried out on a bi-weekly basis. Each measurement was conducted 14 days, give or take 2 days, since the last measurement. The first measurement was done while in quarantine in Chile. The second measurement took place on the Antarctic station on days 5-8 after arrival. Third was done from days 19-22, fourth from days 32 to 40, and fifth from days 48 to 53. The final measurement, the sixth measurement was performed on days 60 to 65.

The first measurement contained the orthostatic test, PVT (psychomotor vigilance task), and IGT (Iowa gambling task). All subsequent measurements included only PVT and IGT.

According to ISO 9886[34], which focuses on the assessment of thermal stress and strain, 14 locations were chosen. These locations according to ISO 9886 are accurate in assessing skin temperatures and establishing mean skin temperature.

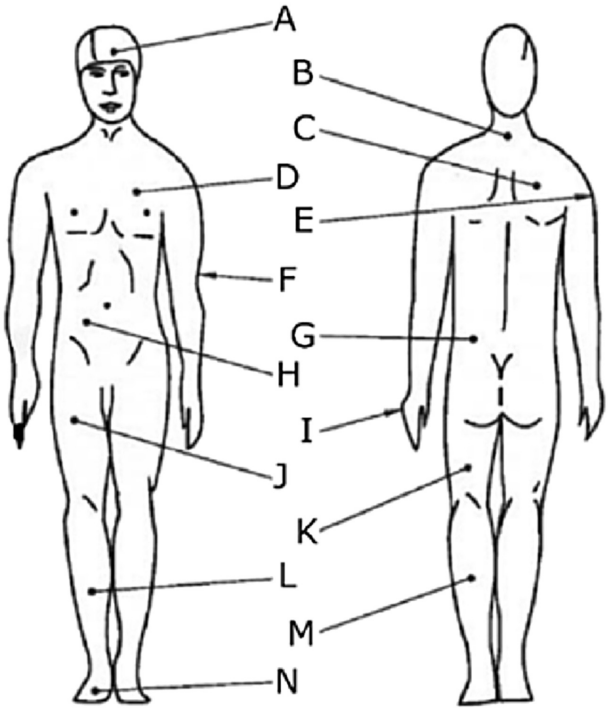

Figure 12: Locations of the ISO defined 14 skin sites for skin temperature measurement [34].

2.3.4 Orthostatic test

Change of position such as from a supine position to a standing position in a gravitation field produces an orthostatic response in the body. In other words, the body has to adjust to the change in blood pressure. During the test blood pressure and heart rate are observed. It may be performed to diagnose orthostatic hypotension in a patient prone to falling when changing positions. The orthostatic test can also be used to test cardio-vascular system recovery after load such as training and lack of sleep. [38]

The participants were instructed to lie down for 4 minutes, then to stand up for 4 minutes, and lastly to lay down again for 4 minutes. Blood pressure measurements were not collected but ECG was performed. The orthostatic test was only included in the first measurement.

2.3.5 Psychomotor Vigilance Task

The Psychomotor Vigilance Task (PVT) is a reaction time test that measures a person's ability to respond quickly to a visual stimulus. [39] The test involves staring at a fixed point on a screen and pressing a button as soon as a stimulus appears on the screen. The test measures how quickly the participant reacts to the stimulus, which is an indicator of their level of alertness, attention, and ability to sustain attention over a period of time. During the experiment, a 5-minute PVT test was administered. A red circle appeared anywhere on a white screen and participants were instructed to press a key as quickly as possible. The reaction time was displayed for about a second after each key press. Intervals between each stimulus were randomized to be between 2 to 10 seconds.

2.3.6 Iowa Gambling Task

The Iowa Gambling Task (IGT) is a psychological task designed to simulate real-life decision-making under conditions of uncertainty. The task involves four decks of cards that are labeled A, B, C, and D. Participants are instructed to choose cards from the decks to maximize their earnings over the course of the task. Unbeknownst to the participants, two of the decks have high rewards but nevertheless also carry high penalties, resulting in a net loss of game currency over time. The other two decks have lower rewards but also carry lower penalties, resulting in a net gain of money over time. Participants were given written instructions. Based on Wemm et al. modification of the IGT [40] the task consisted of 100 selections, when the participant ran out of selections the task ended.

2.4 Pre-processing

Artifacts present in skin temperature sensors were mostly related to kinesio-tape becoming detached. Which resulted in sudden jumps in temperature that could not be explained by underlying physical phenomena. These were usually brief and were replaced after visual inspection utilizing linear interpolation. In case they were longer the whole measurement was excluded from further processing.

All sensors included artifacts when the sensor failed to connect to the receiving device and represented outliers. These resulted in a jump in measured variables but the issue self-corrected in a few seconds. Any such deviation bigger than 10 times the standard deviation was detected, removed, and replaced by a locally weighted scatterplot (LOWESS) smoothing algorithm. LOWESS smoothing was also utilized in removing the data point to data point

variability. This was also helpful in reducing the amount of noise present on the input to the thermophysiological model.

A total of 14 measurements had to be excluded. Sensor data was missing in 6 of the measurements. The recording was cut short in 6 of them. Information about the start and end of each experiment section was missing in 2.

2.5 JOS-3 inputs

The experiment was conceptually divided into several stages which may have different conditions (PAR, position). These correspond to the initial setup (model to equilibrium), the time before the first activity, lying down, standing, lying down, the time before PVT, PVT, the time before IGT, and IGT. The simulation step was chosen to be 1 second to have sufficient detail.

2.5.1 Clothing Insulation

During the experiment, individuals were instructed to put away excess clothing and to be in their underwear if possible. The participants were also instructed that the remainder of the clothes had to be made from cotton. To protect them from cold they could use a sleeping bag to cover portions of their body. Depending on how cold they felt the sleeping bag covered their feet, feet, and lower leg, both of their lower limbs up to the waist, or even up to their shoulders.

Clothing acts as a barrier to heat transfer. It works by reducing air movement between the body and the environment and can reduce thermal radiation as well. For example, wool is a great insulator because it is made up of tiny fibers that trap air pockets between them. Also, the air is a poor conductor of heat. For thermophysiological models estimating the amount of thermal insulation from clothing is paramount.

Clothing insulation is defined by ANSI/ASHRAE Standard 55 as "the resistance to sensible heat transfer provided by a clothing ensemble" [6]. It is usually expressed in clo units, where 1 clo is the amount of insulation required to maintain the thermal comfort of a person at rest in a typical environment (21 °C and 0.1 m/s airspeed). To translate to more familiar unit 1 clo roughly equals 0.155 to $K.m^2.W^{-1}$. Clothing insulation values represent heat insulation from the whole body, that is it assumes that other parts of the body are uncovered.

Conveniently, ANSI/ASHRAE Standard 55 [6] defines clo values for most commonly worn clothes. If two or more pieces of garments are worn it is possible to add their clo values to estimate the combined clothing insulation effects of these garments. Body motion or increased airspeed the body would decrease clothing insulation by increasing the exchange of air between the garment and the body. The experiment was done inside a room with negligible variations in airspeed. Furthermore, it was done on sitting, laying, and standing persons. Therefore clothing insulation values stated in table 5 are for a person who is still.

The sleeping bag used for covering parts of the participant's body was Kilimanjaro Outdoor Adventure Canyon 200. According to the specification, the comfort temperature is +7°C, the

Table 5: Clothing insulation values for garments used during the experiment.

Garment Description	Icl [clo]
Bra	0.01
Panties	0.03
Man's briefs	0.04
T-shirt	0.08
Entrant vest	0.1
Blanket	1.5
Sleeping bag	4

limit temperature is +2 °C and the extreme temperature is -12 °C. The exact value of clo is not known and had to be estimated. This is further complicated by the fact sleeping bags do not usually disclose their clo values and the data on this topic is scarce. According to the review conducted by Mammut [41] the R-value should be 0.4 $K.m^2.W^{-1}$, which translates to 2.5 clo.

The clothing insulation of the vest is also unknown and had to be estimated. It is made out of thick fabric and covers the upper torso leaving the stomach and lower back bare. Using ANSI/ASHRAE Standard 55 it has been estimated to be 0.1 clo.

The blanket type is not known exactly but it was used only once during the whole experiment. Its value was estimated by Henriksson et al. [42] which measured the clo value of a polyester blanket in low airspeeds to be around 1.5 clo.

Finally, the clo value of the chair has to be estimated. Standard 55 states: "A sitting posture results in a decreased thermal insulation due to compression of air layers in the clothing. This decrease may be offset by insulation provided by the chair." [6] It further shows that for many chairs the net effect is minimal and therefore can be disregarded.

2.5.2 Physical Activity Ratio

The physical activity ratio (PAR) represents an individual's physical level. It is calculated by taking the total energy expended during some activity and dividing it by the basal metabolic rate. PAR is a multiple of BMR and as such provides an estimate of how much energy is needed for activity compared to the energy required for basic metabolic functions.

Table 6: Energy cost (PAR) of activities conducted during the experiment.

Activity level	Male	Female
BMR	1.0	1.0
Lying resting	1.2	1.2
Standing resting	1.4	1.5
PVT	1.5	1.64
IGT	1.5	1.64

Physical activity ratios were taken from the Report of a Joint FAO/WHO/UNU [43], which contain PAR ratios for lying and standing for males and females. PAR ratios for PVT and IGT were harder to estimate. They are sedentary tasks performed on a PC but are designed to be demanding psychologically. The most similar category in the FAO report is sitting (office work) with a PAR of 1.5 and playing cards/board games with a PAR of 1.5 as well. Further research revealed this number to be a fairly good approximation. A study from Vermorel et al. [44] measured a variety of activities performed at a desk and found playing video games to have a PAR of approximately 1.5 for males. The data for females is not known and although the PAR tends to differ little between genders close to resting PAR, the PAR for activities tends to differ significantly. A study by Vaz et al. conducted a review and found the relationship to be 0.968 x (Male PAR) + 0.194. For males, a PAR of 1.5 equals 1.65 PAR for females.

2.5.3 Air speed

Although the data on ambient air speed during the experiment is not available it is known the windows remained closed during the experiment and it can reasonably be assumed that air-speed was constant throughout the experiment. ANSI/ASHRAE Standard 55 [6] usually works with values around 0.1 m/s, which JOS-3 also chooses as the reasonably assumed value. Therefore air speed was set to 0.1 m/s.

2.5.4 Initial Conditions

JOS-3 start a simulation with pre-configured conditions which include a set temperature of all nodes not taking into account any specifics such as an individual's physiological characteristics. To bring these conditions in alignment with the actual environmental conditions present during the experiment an extra step had to be taken. The model was initialized with all the variables JOS-3 takes into account and was run for 60 minutes. Allowing the model to reach equilibrium. Ambient conditions for the initial phase were set as the mean of the conditions during the first minute of the experiment data.

2.5.5 Temperature sensors location

In total 14 skin locations were measured during the experiment while there are 17 body segments in JOS-3. Left and right upper limbs were considered to be thermally symmetrical, the same assumption was made for lower limbs. For example, the right shoulder was measured but the left was not, so the temperature in the left shoulder was assumed to be the same as in the right shoulder. Furthermore, there were JOS-3 segments in which the temperature was monitored twice, such as the front of the right thigh and the back of the left thigh. All these instances were averaged together.

3 Results

This chapter is split into two parts, reflecting that there were two experiment designs conducted. The first design contained orthostatic tests in addition to IGT and PVT segments. The second test design contained only PVT and IGT segments. The orthostatic tests were included only during the first measurement which was conducted during quarantine in Chile as opposed to the subsequent 5 measurements which were measured at the Antarctica station.

3.1 Experiment 1

Experiment results for local and mean skin temperatures which included the orthostatic tests can be found in figure 14. The data set comprises 9 measurements. The averaged ambient temperature and ambient humidity conditions during the experiment can be found in figure 13. As can be seen, the overall ambient temperature rises with time and is a result of an effort to keep the participants thermally comfortable since they were wearing only underwear.

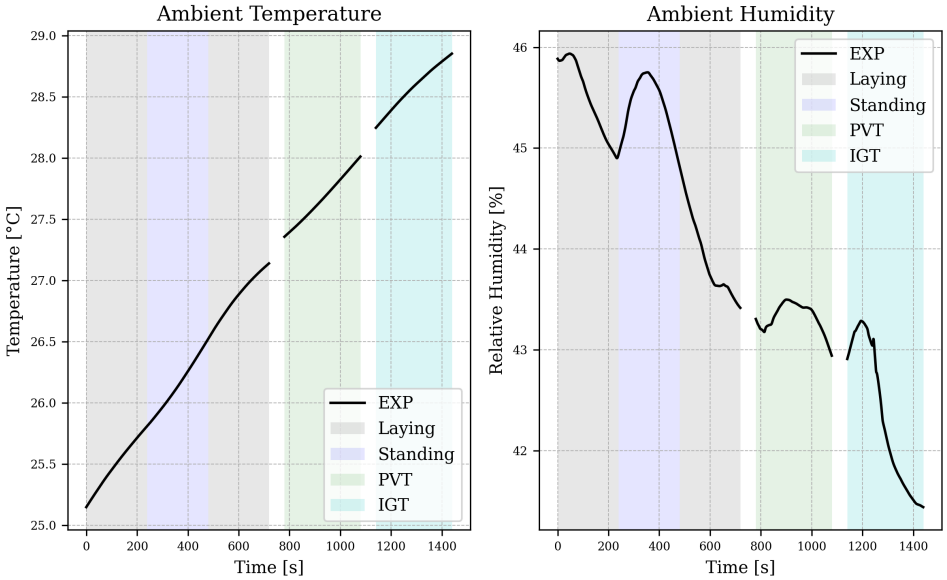

Figure 13: Ambient temperature and humidity during the experiment.

Mean skin temperature was calculated by weighted mean where the weights represent the fraction of the total body surface area each segment represents. Weights were taken from the JOS-3 model in order for the comparison to be meaningful. The overall mean skin temperature RMSD was 0.72 °C.

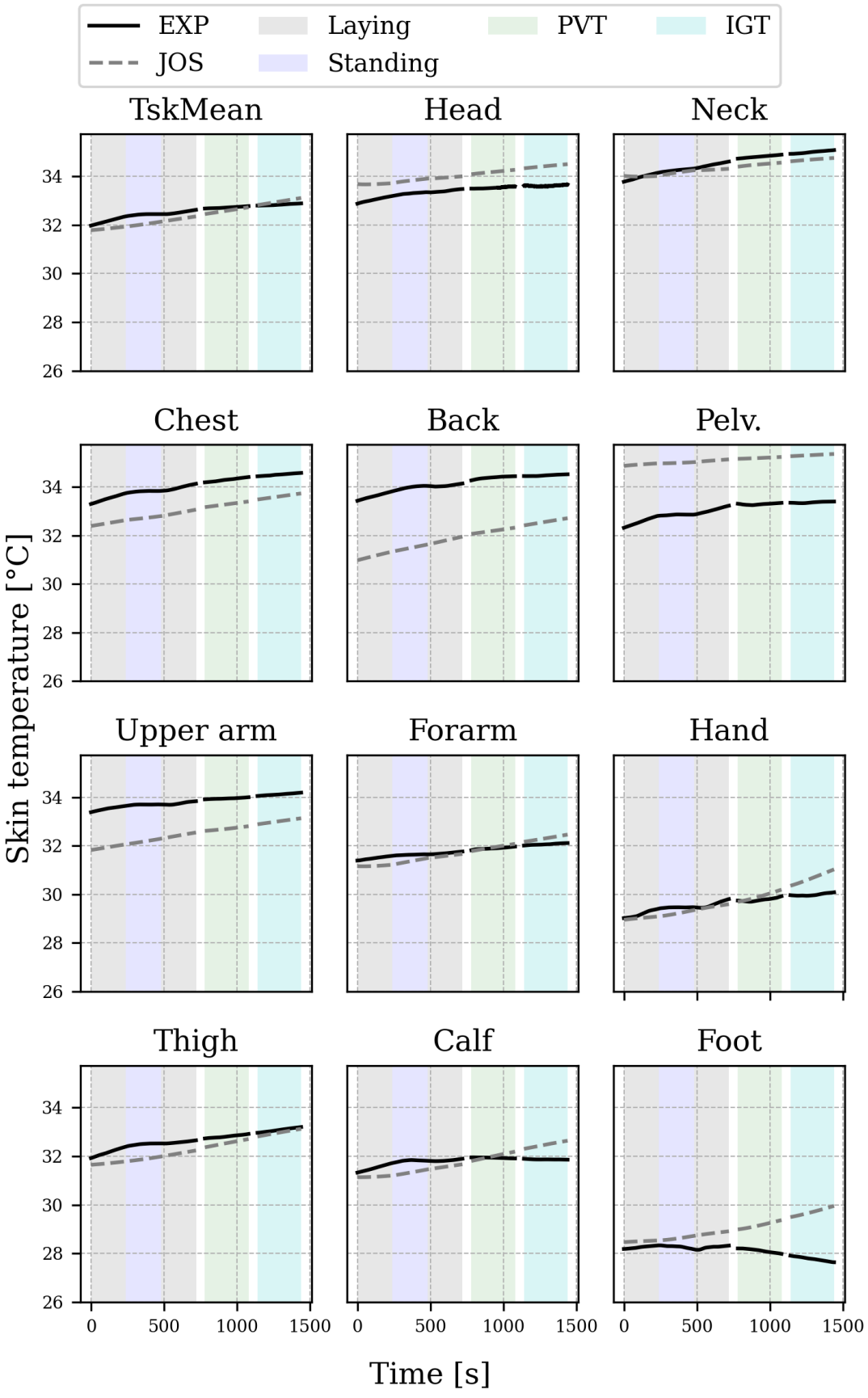

Figure 14: Comparison of measured local skin temperatures and temperatures predicted by JOS-3 model for experiment 1.

An overview of the errors for each segment can be found in table 7. The head segment was overestimated by JOS-3 with ME -0.69 ± 0.22°C. The neck segment showed an overall RMSD of 0.61 °C which is the lowest of the segments, the ME was 0.12 ± 0.27 °C showing little overall model underestimation or overestimation. The chest segment was underestimated by JOS-3 by 0.97 ± 0.18°C. The back and pelvis show two of the highest RMSD of 2.25 and 2.18 °C respectively. Although the back was underestimated by 2.23 ± 0.28°C, the pelvis on the other hand was overestimated by 2.15 ± 0.35°C.

Table 7: Overview of the errors between experimental data and predicted values by JOS-3 for experiment design 1.

Segment	ME	SD	MAE	RMSD
Mean skin	0.13	0.22	0.67	0.72
Head	-0.69	0.21	0.78	0.82
Neck	0.12	0.27	0.56	0.61
Chest	0.97	0.18	0.99	1.01
Back	2.23	0.28	2.23	2.25
Pelvis	-2.15	0.35	2.15	2.18
Upper arm	1.3	0.21	1.38	1.4
Forearm	0.03	0.31	1.42	1.48
Hand	-0.15	0.73	1.95	2.08
Thigh	0.32	0.25	0.67	0.71
Calf	-0.02	0.48	1.01	1.1
Foot	-0.98	0.8	1.96	2.13

Higher limbs had RMSD of 1.4, 1.48, and 2.08 °C for the upper arm, forearm, and hand respectively. Forearm and hand were neither significantly overestimated nor underestimated showing MA 0.03 ± 0.31°C and -0.15 ± 0.73°C. The upper arm was constantly underestimated by 1.3 ± 0.21°C. A trend can be observed in figure 14. The trend shows that during PVT and IGT all higher limb segments show an increase in temperature that is not reflected in measured data.

Lower limbs had RMSD of 0.71, 1.1, and 2.13 °C for thigh, calf, and foot segments respectively. The trend, which was also present in the upper limbs, shows a steady temperature increase in the JOS-3 model that is not reflected in the data. This is especially pronounced in the calf and foot segment where the temperature decreases during PVT and IGT. The participants were only in their underwear and did not wear sleeping bag on their lower limbs which was only present in later measurements.

3.2 Experiment 2

Experiment results containing mean skin temperature during IGT and PVT segments can be found in figure 15. The data set consists of 70 measurements. The overall mean skin tempera-

ture RMSD was 0.75 °C.

Figure 15 shows that during the first 100 seconds, the JOS-3 modeled mean skin temperature is overestimated by less than 0.1 °C from the data obtained during the experiment. By the end of the IGT segment, the mean skin temperature is overestimated by JOS-3 by more than 0.4 °C. The IGT segment was measured immediately after PVT, nevertheless set up for the next test, and explaining of rules usually took 30-90 seconds. This is why there is a gap between PVT and IGT on this and all further graphs.

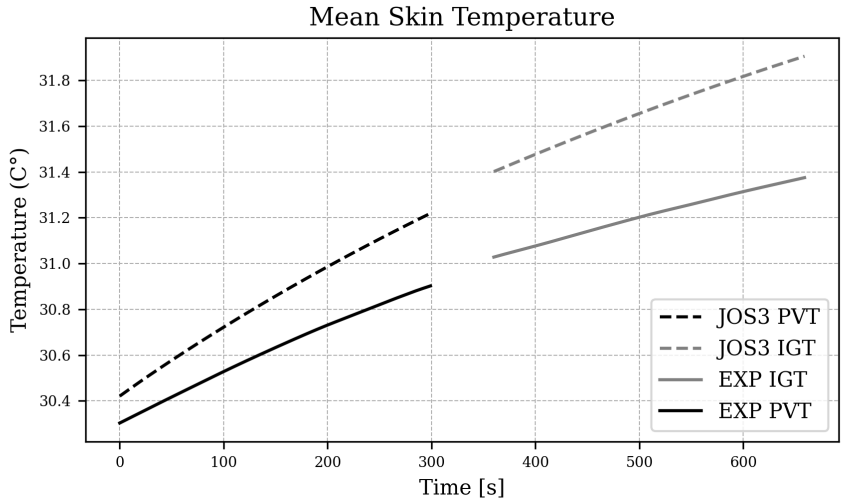

Figure 15: Mean skin temperature during PVT and IGT segments.

The ambient environmental conditions during the experiment can be seen in figure 16. The temperature rise is a consequence of increasing the central heating setting. This was done to keep the participants thermally comfortable since they mostly wore only underwear and potentially a sleeping bag had a sleeping bag from lower limbs up to where they felt they would be thermally comfortable during the experiment.

Figure 17 shows the experimental results for local skin temperatures and their corresponding JOS-3 predicted temperatures during PVT and IGT segment. The figure contains only one limb out of two since the error is the same for the left and right limbs.

An overview of the errors between measured data and the predicted values of JOS-3 for all segments can be seen in table 8. The RMSD for the head, neck, and chest is close to 1. Figure 17 shows that JOS-3 overestimated head, neck, and calf segment skin temperatures by 0.97 ± 0.31 °C, 0.6 ± 0.41 °C, and 0.74 ± 0.45 °C respectively. It significantly overestimated thigh skin temperature by 1.78 ± 0.53 °C. The pelvis was overestimated by 3.96 ± 0.16 °C. The pelvis also had the highest RMSD error of 3.96 °C of all the segments.

Skin temperatures were mildly underestimated in chest and forearm segments by 0.76 ± 0.24 °C and 0.6 ± 0.19 °C respectively. Significantly underestimated were upper arm, hand, and foot segments by 1.87 ± 0.2 °C, 1.62 ± 0.54 °C, and 1.69 ± 0.41 °C respectively. Back skin temperature was the most underestimated by the JOS-3 model by 2.3 ± 0.22 °C. The back, hand, and foot had all RMSD close to 2.5 °C.

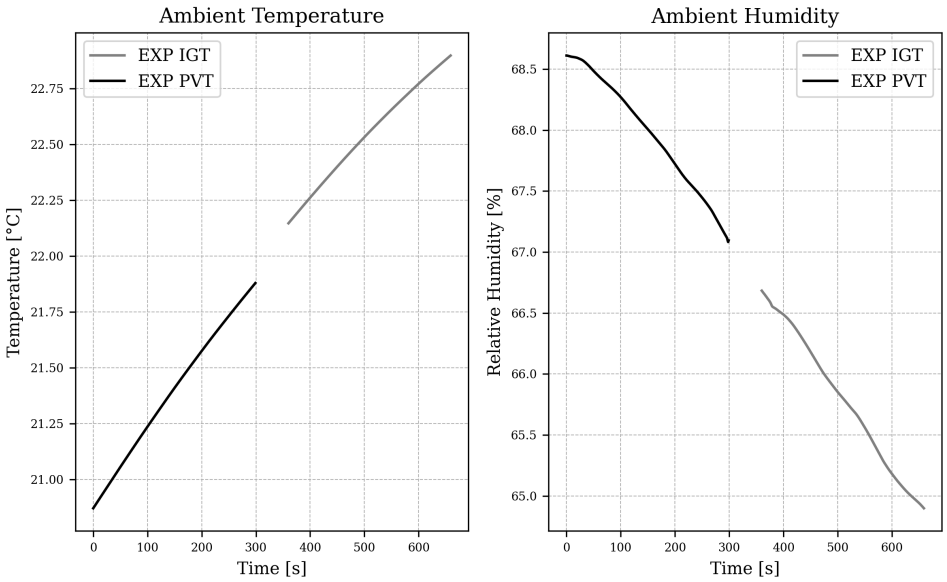

Figure 16: Ambient temperature and humidity during the experiment

Table 8: Overview of the errors between experimental data and predicted values by JOS-3.

Segment	ME	SD	MAE	RMSD
Mean skin	-0.34	0.2	0.72	0.75
Head	-0.97	0.31	1.07	1.13
Neck	-0.6	0.41	0.92	1
Chest	0.76	0.24	1.18	1.22
Back	2.3	0.22	2.53	2.55
Pelvis	-3.96	0.16	3.96	3.96
Upper arm	1.87	0.2	1.9	1.92
Forearm	0.6	0.19	0.95	0.97
Hand	1.62	0.54	2.61	2.68
Thigh	-1.78	0.53	1.97	2.04
Calf	-0.83	0.61	1.35	1.45
Foot	1.69	0.41	2.62	2.67

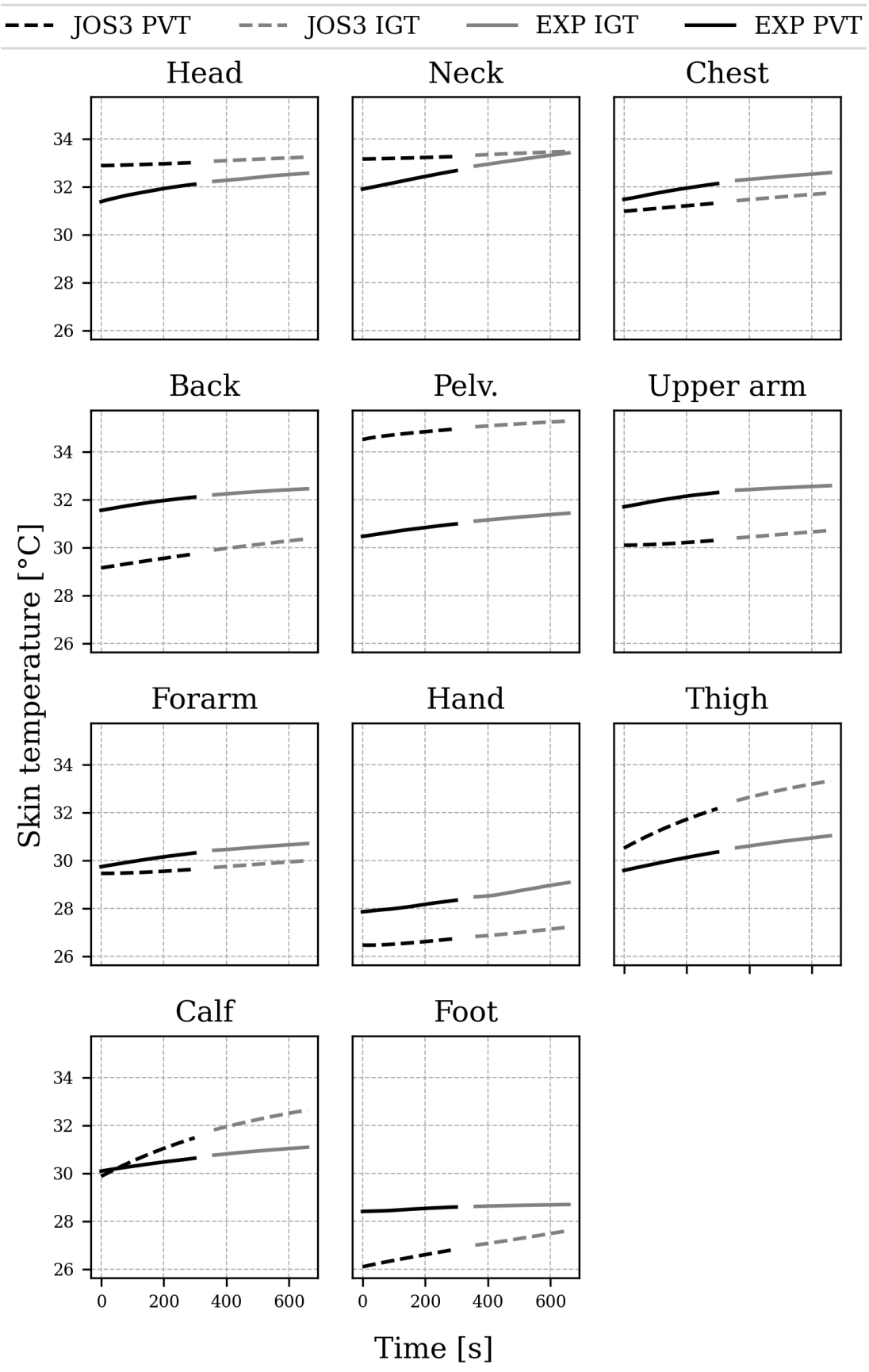

Figure 17: Comparison of measured local skin temperatures and temperatures predicted by JOS-3 model for experiment 2.

Due to the uncertainty of the insulation clothing value of the sleeping bag and the noticeable JOS-3 trend in thigh, calf, and foot segments, the simulation was run again. The clothing value selected was 2, which corresponds to a lighter sleeping bag according to Mammut [41]. Furthermore, a clo value of 1 was chosen for comparison.

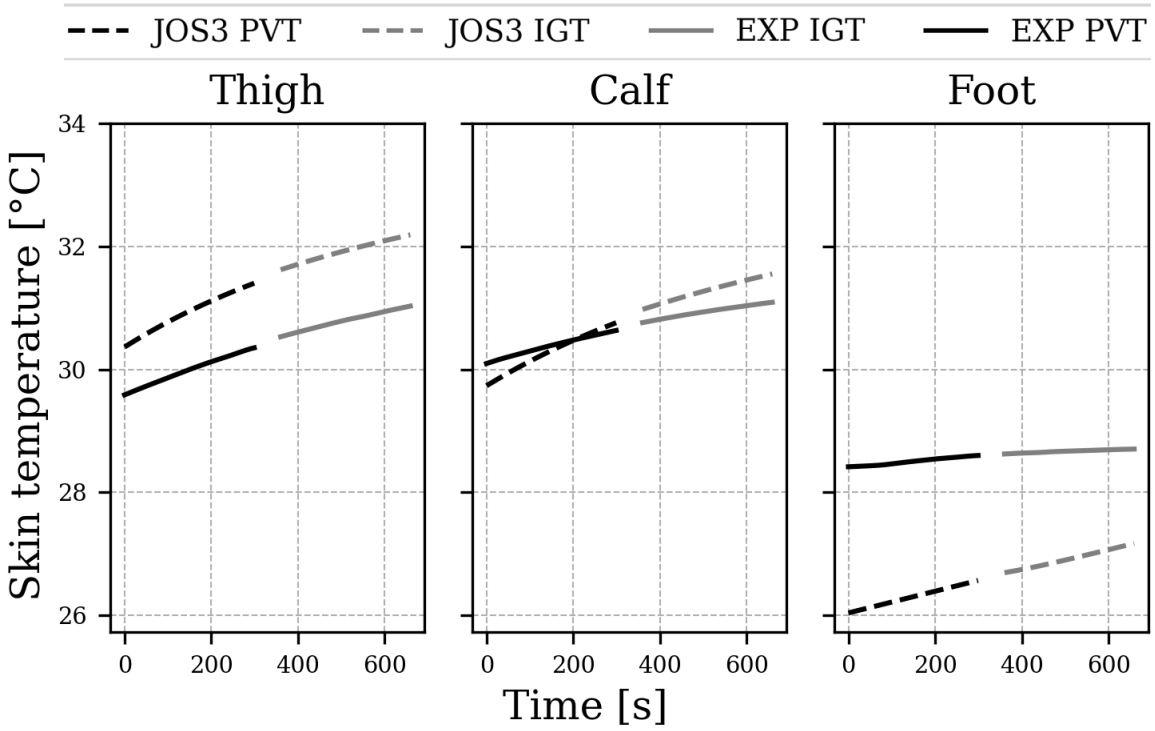

Figure 18: Decreasing sleeping bag clothing insulation to 1 for lower limbs segments.

The thigh and calf segments show an improvement in RMSD with decreasing clo values. For the thigh segment, the RMSD is 1.71 and 1.36 for clo values of 2 and 1 respectively. For the calf segment, the RMSD is 1.2 and 0.98 for the clo value of 2 and 1 respectively. As the foot segment is underestimated in JOS-3 the RMSD increased when decreasing clo values. The trend for a clothing insulation value of 2 still shows a noticeable trend and is therefore not shown. For the clo value of 1, the trend is comparable to the trend obtained from actual experiment data and can be seen in 18.

4 Discussion

Prediction of mean skin temperature

The JOS-3 model showed good accuracy (RMSD = 0.72 °C and RMSD = 0.75 °C for experiments 1 and 2 respectively) when predicting the overall mean skin temperature across all participants. The RMSD error is comparable with previous validation results done by Takahashi et. al [12], which found an average RMSD of 0.5 °C for steady-state conditions and RMSD of 0.58 - 0.83 °C for transient conditions. The mean error was 0.13 ± 0.22 °C -0.34 ± 0.3 °C for experiments 1 and 2 respectively, indicating that on average JOS-3 predictions were not overestimated or underestimated.

The agreement between modeled and measured local skin temperatures was variable. The head, neck, and chest, displayed overall RMSD from 0.61 - 1.22 °C across both experiments. While other segments displayed relatively higher RMSD values. Exploration into possible causes will be discussed below. For comparison, the range of RMSD for all local skin temperatures done by Takahashi et. al [12] for steady-state conditions was 0.57 - 1.77 °C, results for transient conditions are not available.

Prediction of pelvis temperature

The mean pelvis skin temperature is greatly overestimated by JOS-3 (ME = -2.15 ± 0.35 °C for experiment 1, ME = -3.96 ± 0.16 °C for experiment 2). Even though the participants frequently had the sleeping bag up their lower stomachs, such a deviation cannot be explained by uncertainty of the clothing insulation value of the sleeping bag. Furthermore, if that was the case it would be expected that the deviation starts relatively low and grows with time as can be seen in thigh or calf segments during experiment 2. This is not the case since the deviation starts close to the mean error.

The mean measured pelvis temperature for all participants is 32.95 ± 0.49 °C and 31 ± 0.32 °C for experiment 1 and 2 respectively. While the ambient temperature during experiment 1 was typically between 25 - 29 °C and 20 - 23 °C for experiment 2. A study by Foda et. al [45] measured the skin temperatures of 11 participants during steady-state conditions of 25 °C and found the mean pelvis temperature to be 33 ± 0.77 °C. The measurement time was 1h. Participants wore office clothing. Although slightly higher it shows the measured pelvis temperatures are not unreasonably low. Furthermore, in the original paper by Takahashi et al. which introduced the JOS-3 model, JOS-3 was also validated in an experiment by Werner and Reents [14] which measured skin temperatures in steady-state conditions. The average pelvis temperature was around 31 and 34 °C for steady-state temperatures of 20 °C and 30 °C

respectively. The values are not precise as they were taken from figures. The JOS-3 model results indicate that the pelvis was slightly overestimated by the model but no more than 0.5 °C for both steady-state conditions for the experimental conditions measured by Werner and Reents. The previous results reported in the study could not be replicated. All of the coefficients and equations have been checked but the discrepancy was not resolved. Authors of the JOS-3 model were made aware of the discrepancy.

Prediction of lower limbs temperatures - clothing insulation

For thigh, calf, and foot the RMSD during experiment 2 was 2.04 °C, 1.45 °C, and 2.67 °C. For experiment 1 the RMSD was 0.71 °C, 1.1 °C, 2.13 °C. Higher RMSD errors in lower limbs during experiment 2 may be partially explained by the uncertainty of the actual clothing insulation value of the sleeping bag. The RMSD of the foot segment remains high between experiments 1 and 2 and other possible causes will be explained section in another section.

Participants had the sleeping bag up to the top of their thighs in around 65 % of the measurements. As can be seen in figure 17 thigh and calf segments seem to start with very little deviation from the measured value but the deviation grows with time. A possible explanation for the thigh and calf segments is that either JOS-3 overestimates the actual importance of higher clothing insulation values or that the actual clothing insulation value was overestimated. Further experiments have shown that the trend significantly decreases when using lower clothing insulation values of 2 and 1. The overestimation of the clothing value can be a result of the unavailability of exact clothing insulation values for the type of sleeping bag used. For further measurements, it is advisable to use a piece of clothing with known clothing insulation value.

Another possible explanation is that JOS-3 models clothing insulation as a thermal resistance only and ignores the possible effect of heat capacity and moisture absorption of used clothing. The heat capacity and moisture absorption of the sleeping bag for example may not be insignificant compared to other commonly worn clothing ensembles and could act as a heat sink in the initial moments of the measurement.

Prediction of back temperature

The back skin temperature is overestimated is underestimated by JOS-3 in experiment 1 (ME = 2.23 ± 0.28 °C, RMSD = 2.25 °C) and also in experiment 2 (ME = 2.3 ± 0.22 °C, RMSD = 2.55 °C). The difference is too great to be explained by uncertainty in the clothing insulation of the Entrant vest. Taking the second experiment as an example the temperatures were typically between 21 - 23 °C for these ranges the measured mean back skin temperature was 32.08 ± 0.3 °C. JOS-3 was validated by an experiment by Werner and Reents [14] which included steady-state conditions for 20 °C and 30 °C, the measured back temperatures were about 28 and 34 °C respectively. The exact placement of the sensor is not published. The predictions by JOS-3 were well within 0.5 °C RMSD for both conditions. In comparison a study by Foda et. al [45] measured the skin temperatures of 11 participants during steady-state conditions of

25 °C and found the back temperature to be 34.72 ± 1.15 °C. The result was obtained as an average from 4 locations, the left and right scapula and the left and right side of the lower back. Participants wore normal office clothes.

Ultimately, since the location of sensors is not standardized the comparison of the resulting measurements is difficult. These might not be an issue with locations such as the head, where the most usual placement is the forehead, and neck, where the sensor is almost always placed on cervical vertebrae below hairline. Nevertheless, for substantial areas such as back standardization may be needed.

Prediction of hand and foot temperatures

The JOS-3 model underestimated skin temperature during experiment 2 in the hand (ME = 1.62 ± 0.54 °C, RMSD = 2.68 °C) and foot segment (ME = 1.69 ± 0.41 °C, RMSD = 2.67 °C). During experiment 1 the errors were for hand (ME = -0.15 ± 0.73 °C, RMSD = 2.08 °C) and foot segment (ME = -0.98 ± 0.8 °C, RMSD = 2.13 °C). Although the RMSD errors remained high across the experiments the mean error changed significantly. Noteworthy is also the fact that the mean error standard deviation was one of the highest compared to other segments, except for the foot segment during experiment 2. During experiment 2 the segment was usually located inside the sleeping bag which might have influenced the variability.

A possible explanation may be that the temperature variability between the location of the thermal sensor and the rest of the segment in hand and feet is significant. The JOS-3 model gives a temperature output for the whole segment. For example, a study by Leijon-Sundqvist et al. [46] studied dorsal and palmar hand temperatures in 112 participants via infrared camera. The study found that the temperatures in fingers can vary by several °C to the temperature measured on the dorsal side between knuckles and wrist.

Another source of inaccuracies could be that hand and feet may be in contact with surfaces such as table or floor. In experiment 1 the measured foot temperature can be seen decreasing during PVT and IGT, while other skin temperatures are rising. This could be explained by heat transfer to the floor. Same phenomena, although less pronounced, can be observed for measured hand temperatures during PVT and IGT in experiment 1.

Limitations

The measurement length was on a relatively shorter timescale when compared to other studies validating and comparing thermophysiological models. The duration of each measurement was usually between 11-20 minutes. Furthermore, there was no initial phase of the measurement which would allow the participants' temperature to get accustomed to the environmental conditions of the room experiments were conducted in, and the clothing ensembles worn during the experiment. Another limitation is uncertainty in clothing insulation value of the sleeping bag used during experiment.

Future works

Follow-up research studies should include a 30-60 minutes adaptation phase before the experiment. Although the participant does not have to be measured, environmental conditions should be recorded and the participant should be already wearing clothes that will be worn during an experiment and not do physically demanding tasks. Furthermore, standardized clothing should be worn with known clothing insulation values.

5 Conclusion

Based on a literary review of thermophysiological models 4 matched the broader criteria and were selected for further comparison. From the comparison of the models JOS-3 model was selected as the most suitable, chiefly since it may take into consideration all the individual physiological characteristics collected during the experiment during the longitudinal experiment in Antarctica, was widely validated and recognized in the field, and was open source (included all the details for its implementation and or modifications).

The JOS-3 model was applied to the two main experiment designs. The overall mean skin temperature (RMSD 0.72 °C and 0.75 °C for experiments 1 and 2 respectively) falls within the range of values reported by the JOS-3 paper. RMSD for individual segments were mixed but were within RMSD of 1.22 °C for head, neck, and chest segments. The possible causes for some of the higher RMSD of each segment were discussed and possible future experiment improvements were suggested.

This thesis showed that even with experiment designs utilizing shorter observation periods mean skin temperatures can be reliably modeled with JOS-3 thermophysiological model.

Bibliography

[1] D. Fiala, “Dynamic simulation of human heat transfer and thermal comfort,” De Montfort University, 1998.

[2] W. D. van Marken Lichtenbelt and P. Schrauwen, “Implications of nonshivering thermogenesis for energy balance regulation in humans,” *American Journal of Physiology - Regulatory Integrative and Comparative Physiology*, vol. 301, pp. 285–296, 2 Aug. 2011, ISSN: 03636119. DOI: 10.1152/ajpregu.00652.2010.

[3] S. Lazzer and G. O’Malley, “Metabolic and mechanical cost of sedentary and physical activities in obese children and adolescents,” *The ECOG’s eBook on Child and Adolescent Obesity*, 2015.

[4] M. Calcagno, H. Kahleova, J. Alwarith, *et al.*, “The thermic effect of food: A review,” *Journal of the American College of Nutrition*, vol. 38, pp. 547–551, 6 Aug. 2019, ISSN: 15411087. DOI: 10.1080/07315724.2018.1552544.

[5] C. Jessen, “Physics of heat exchange with the environment,” *Temperature Regulation in Humans and Other Mammals*, pp. 37–46, 2001. DOI: 10.1007/978-3-642-59461-8_6.

[6] ANSI/ASHRAE, *Standard 55: Thermal Environmental Conditions for Human Occupancy*. American Society of Heating, Refrigerating and Air-Conditioning Engineers Inc.: Atlanta, 2010.

[7] J. Hensen, “On the thermal interaction of building structure and heating and ventilating system,” Technische Universiteit Eindhoven, 1991. DOI: 10.6100/IR353263.

[8] N. Djongyang, R. Tchinda, and D. Njomo, “Thermal comfort: A review paper,” *Renewable and Sustainable Energy Reviews*, vol. 14, 9 2010, ISSN: 13640321. DOI: 10.1016/J.RSER.2010.07.040.

[9] H. H. Pennes, “Analysis of tissue and arterial blood temperatures in the resting human forearm,” *Journal of applied physiology*, vol. 1, pp. 93–122, 2 Aug. 1948, ISSN: 00218987. DOI: 10.1152/JAPPL.1948.1.2.93.

[10] J. A. Stolwijk and J. B. Pierce, “A mathematical model of physiological temperature regulation in man,” National Aeronautics and Space Administration, 1971.

[11] K. Katić, R. Li, and W. Zeiler, “Thermophysiological models and their applications: A review,” *Building and Environment*, vol. 106, pp. 286–300, Sep. 2016, ISSN: 0360-1323. DOI: 10.1016/J.BUILDENV.2016.06.031.

[12] Y. Takahashi, A. Nomoto, S. Yoda, *et al.*, "Thermoregulation model jos-3 with new open source code," *Energy and Buildings*, vol. 231, Jan. 2021, ISSN: 03787788. DOI: 10.1016/J.ENBUILD.2020.110575.

[13] B. Kingma, "Human thermoregulation; a synergy between physiology and mathematical modeling," Jan. 2012. DOI: 10.26481/DIS.20120227BK.

[14] J. Werner and T. Reents, "A contribution to the topography of temperature regulation in man," *European journal of applied physiology and occupational physiology*, vol. 45, pp. 87–94, 1980. DOI: 10.1007/BF00421205.

[15] J. D. Hardy and J. A. Stolwijk, "Partitional calorimetric studies of man during exposures to thermal transients," *Journal of Applied Physiology*, vol. 21, pp. 1799–1806, 6 1966, ISSN: 00218987. DOI: 10.1152/JAPPL.1966.21.6.1799.

[16] J. A. J. Stolwijk and J. A. Hardy, "Partitional calorimetric studies of responses of man to thermal transients.," *Journal of Applied Physiology*, vol. 21, pp. 967–977, 3 1966, ISSN: 00218987. DOI: 10.1152/JAPPL.1966.21.3.967.

[17] R. Amare, A. A. Bahadori, and S. Eckels, "A structured cleaving mesh for bioheat transfer application," *IEEE Open Journal of Engineering in Medicine and Biology*, vol. 1, pp. 174–186, 2020, ISSN: 26441276. DOI: 10.1109/OJEMB.2020.2994557.

[18] B. Givoni and R. F. Goldman, "Predicting metabolic energy cost.," *Journal of Applied Physiology*, vol. 30, pp. 429–433, 3 1971, ISSN: 00218987. DOI: 10.1152/jappl.1971.30.3.429.

[19] A. Gagge, J. A. Stolwijk, and Y. Nishi, "An effective temperature scale based on a simple model of human physiological response," *ASHRAE Trans. 77*, pp. 247–262, 1971.

[20] B. W. Jones, "Transient interaction between the human and the thermal environment," *ASHRAE Trans.*, vol. 98, pp. 189–195, 1 1992.

[21] S. I. Tanabe, K. Kobayashi, J. Nakano, Y. Ozeki, and M. Konishi, "Evaluation of thermal comfort using combined multi-node thermoregulation (65mn) and radiation models and computational fluid dynamics (cfd)," *Energy and Buildings*, vol. 34, pp. 637–646, 6 Jul. 2002, ISSN: 03787788. DOI: 10.1016/S0378-7788(02)00014-2.

[22] C. Huizenga, H. Zhang, and E. Arens, "A model of human physiology and comfort for assessing complex thermal environments," *Elsevier*, vol. 36, pp. 691–699, 2001. DOI: 10.1016/S0360-1323(00)00061-5.

[23] E. H. Wissler *et al.*, "Mathematical simulation of human thermal behavior using whole body models," *Heat transfer in medicine and biology*, vol. 1, pp. 325–373, 13 1985.

[24] X. Sun, S. Eckels, and Z. C. Zheng, "An improved thermal model of the human body," *Hvac and Research*, vol. 18, pp. 323–338, 3 2012.

[25] Y. Tang, Y. He, H. Shao, and C. Ji, "Assessment of comfortable clothing thermal resistance using a multi-scale human thermoregulatory model," *International Journal of Heat and Mass Transfer*, vol. 98, pp. 568–583, 2016.

[26] R. Streblow, "Thermal sensation and comfort model for inhomogeneous indoor environments," ISBN: 978-3-942789-00-4.

[27] N. Martínez, A. Psikuta, K. Kuklane, *et al.*, "Validation of the thermophysiological model by fiala for prediction of local skin temperatures," *International Journal of Biometeorology*, vol. 60, pp. 1969–1982, 12 Dec. 2016, ISSN: 00207128. DOI: 10.1007/S00484-016-1184-1.

[28] H. Zhang, C. Huizenga, E. Arens, and T. Yu, "Considering individual physiological differences in a human thermal model," *Journal of Thermal Biology*, vol. 26, pp. 401–408, 4-5 Sep. 2001, ISSN: 0306-4565. DOI: 10.1016/S0306-4565(01)00051-1.

[29] "A heat health hazard index based on ecmwf data | ecmwf." Accessed on March 17, 2023. (2020), [Online]. Available: https://www.ecmwf.int/en/newsletter/162/news/heat-health-hazard-index-based-ecmwf-data.

[30] D. Fiala, G. Havenith, P. Bröde, B. Kampmann, and G. Jendritzky, "Utci-fiala multi-node model of human heat transfer and temperature regulation," *International journal of biometeorology*, vol. 56, pp. 429–441, 3 2012, ISSN: 1432-1254. DOI: 10.1007/S00484-011-0424-7.

[31] D. Fiala, A. Psikuta, G. Jendritzky, *et al.*, "Physiological modeling for technical, clinical and research applications," *Frontiers in Bioscience-scholar*, vol. 2, pp. 939–968, 3 2010. DOI: 10.2741/S112.

[32] T. R. Miller, D. A. Nelson, L. Kuznetz, and G. Bue, "Dynamic simulation of human thermoregulation and heat transfer for spaceflight applications," *41st International Conference on Environmental Systems 2011, ICES 2011*, 2011. DOI: 10.2514/6.2011-5083.

[33] F. Zlámal, P. Lenart, D. Kuruczová, *et al.*, "Stress entropic load: New stress measurement method?" *PLOS ONE*, vol. 13, e0205812, 10 Oct. 2018, ISSN: 1932-6203. DOI: 10.1371/JOURNAL.PONE.0205812.

[34] ISO, "9886:2004 - ergonomics — evaluation of thermal strain by physiological measurements," International Organization for Standardization, 2004.

[35] A. Zolfaghari and M. Maerefat, "A new simplified thermoregulatory bioheat model for evaluating thermal response of the human body to transient environments," *Building and Environment*, vol. 45, pp. 2068–2076, 10 Oct. 2010, ISSN: 03601323. DOI: 10.1016/J.BUILDENV.2010.03.002.

[36] Y. Kobayashi and S. I. Tanabe, "Development of jos-2 human thermoregulation model with detailed vascular system," *Building and Environment*, vol. 66, pp. 1–10, Aug. 2013, ISSN: 03601323. DOI: 10.1016/J.BUILDENV.2013.04.013.

[37] Y. Inoue, M. Nakao, T. Araki, and H. Ueda, "Thermoregulatory responses of young and older men to cold exposure," *European journal of applied physiology and occupational physiology*, vol. 65, pp. 492–498, 6 Nov. 1992, ISSN: 0301-5548. DOI: 10.1007/BF00602354.

[38] A. Fanciulli, N. Campese, and G. K. Wenning, "The schellong test: Detecting orthostatic blood pressure and heart rate changes in german-speaking countries," *Clinical Autonomic Research*, vol. 29, pp. 363–366, 4 Aug. 2019, ISSN: 16191560. DOI: 10.1007/S10286-019-00619-7/FIGURES/1.

[39] M. Basner and D. F. Dinges, "Maximizing sensitivity of the psychomotor vigilance test (pvt) to sleep loss," *Sleep*, vol. 34, p. 581, 5 May 2011, ISSN: 15509109. DOI: 10.1093/SLEEP/34.5.581.

[40] S. E. Wemm and E. Wulfert, "Effects of acute stress on decision making," *Applied psychophysiology and biofeedback*, vol. 42, pp. 1–12, 1 Mar. 2017, ISSN: 1573-3270. DOI: 10.1007/S10484-016-9347-8.

[41] Mammut. "Sleep well part 1 | temperature ratings a review of temperature standards for sleeping bags." (2006), [Online]. Available: http://activelife.dp.ua/files/Mammut_Sleep_well_pt1_E.pdf.

[42] O. Henriksson, J. P. Lundgren, K. Kuklane, I. Holmér, and U. Bjornstig, "Protection against cold in prehospital care - thermal insulation properties of blankets and rescue bags in different wind conditions," *Prehospital and Disaster Medicine*, vol. 24, pp. 408–415, 5 2009, ISSN: 19451938. DOI: 10.1017/S1049023X00007238.

[43] M. Vaz, N. Karaolis, A. Draper, and P. Shetty, "A compilation of energy costs of physical activities," *Public Health Nutrition*, vol. 8, pp. 1153–1183, 7a Oct. 2005, ISSN: 1475-2727. DOI: 10.1079/PHN2005802.

[44] M. Vermorel, S. Lazzer, A. Bitar, *et al.*, "Contributing factors and variability of energy expenditure in non-obese, obese, and post-obese adolescents," *Reproduction Nutrition Development*, vol. 45, pp. 129–142, 2 Mar. 2005, ISSN: 09265287. DOI: 10.1051/RND:2005014.

[45] E. Foda, "Evaluating local and overall thermal comfort in buildings using thermal manikins," Aalto University, 2012, ISBN: 978-952-60-4815-4.

[46] K. Leijon-Sundqvist, Y. Tegner, F. Olsson, K. Karp, and N. Lehto, "Relation between dorsal and palmar hand skin temperatures during a cold stress test," *Journal of Thermal Biology*, vol. 66, pp. 87–92, May 2017, ISSN: 0306-4565. DOI: 10.1016/J.JTHERBIO.2017.04.003.

List of Figures

List of Tables

List of Abbreviations

ADMR	Average Daily Metabolic Rate
ANSI	American National Standards Institute
ASHRAE	American Society of Heating, Refrigerating and Air-Conditioning Engineers
AVA	Arteriovenous Anestomoses
BAT	Brown Adipose Tissue
BMR	Basal Metabolic Rate
BMI	Body Mass Index
ISO	International Organization for Standardization
IGT	Iowa Gambling Task
LOWESS	Locally Weighted Scatterplot Smoothing
NASA	National Aeronautics and Space Administration
MAE	Mean Absolute Error
ME	Mean Error
PAR	Physical Activity Ratio
PVT	Psychomotor Vigilance Task
RMSD	Root Mean Square Deviation
SD	Standard Deviation
TEF	Thermic Effect of Food
UTCI	Universal Thermal Climate Index